THE SHORT-TERM EFFECTS OF DIABETES ON THE EXPRESSION AND FUNCTION OF TETRODOTOXIN-SENSITIVE VOLTAGE-GATED SODIUM CHANNELS IN MOUSE SENSORY NEURONS

A Thesis Submitted to the College of Graduate and Postdoctoral Studies
In Partial Fulfillment of the Requirements for the Degree of Master of Science
In the Department of Anatomy, Physiology and Pharmacology (APP)
University of Saskatchewan, Saskatoon, SK

By

MARICRIS NARVATO BAUTISTA

PERMISSION TO USE

By presenting this thesis in partial fulfillment of the requirements for a postgraduate degree from the University of Saskatchewan, I permit the libraries of this university may make it freely available for appraisal. I further agree that permission for copying of this thesis in any manner, either wholly or partially for scholarly purposes may be granted by the supervisor or committee members who supervised my work, or in their absence, by the Head of the Department or Dean of the College in which my thesis was completed. It is understood that the copying or publication of this thesis wholly or parts thereof for financial gain will not be allowed without my written permission. It is also understood that due recognition will be given to me and to the University of Saskatchewan in any scholarly use which may be produced from any material contained in my thesis.

Requests for permission to copy of make other use from material in this thesis either wholly or partially must be addressed to:

Head of the Department of Anatomy, Physiology and Pharmacology (APP)
College of Medicine
University of Saskatchewan
Saskatoon, Saskatchewan S7N 5E5

Dean
College of Graduate and Postdoctoral Studies
University of Saskatchewan
116 Thorvaldson Building, 110 Science Place
Saskatoon SK S7N 5C9

ABSTRACT

Diabetic Sensory Neuropathy (DSN) presents with a constellation of sensory abnormalities, including numbness, tingling sensations, exacerbated responses to painful and non-painful stimuli, and a paradoxical loss of pain sensation. Despite the substantial burden that DSN afflicts on patients, the underlying mechanisms contributing to the pathogenesis of this disorder remains poorly understood. Particular interest has been concentrated on voltage-gated sodium (Nav) channels, especially their roles in painful forms of neuropathies in long-term diabetes. However, their possible contributions to the onset of neuropathy are still under investigation.

This project aimed at elucidating the roles of Nav channels during the early stages of DSN in sensory neurons from the dorsal root ganglion (DRG). We used cultured DRG neurons, maintained in either control (5 mM glucose) or in high glucose media (25 mM) for up to 14 days for patch-clamp electrophysiology. In addition, we used intact DRG tissues from streptozotocin (STZ)-induced diabetic mice, at one and three months after diabetes induction for the detection of Nav subunit expression. Our results indicate that DRG neurons maintained in high glucose show reduced action potential firing frequency and reduced inward currents. In addition, we observed a significant downregulation in the TTX-S Nav1.3, Nav1.6, and Nav1.7 subunits in intact DRG tissues from one-month STZ-diabetic mice. The Navβ2 subunit, which has been shown to regulate the cell surface expression of TTX-S Nav channels, also shows statistically significant reductions in its expression levels. Interestingly, after three months of STZ-induced diabetes, there was a significant upregulation in the expression level of the TTX-S Nav1.7 subunit. Taken together, our data reveal that changes causing reduction of expression and function of TTX-S Nav subunits take place at early stages in diabetes, while increased expression in Nav subunits occurs later in the disease. Therefore, our data suggest a potential role for Nav subunits in the development of the various sensory symptoms in DSN.

ACKNOWLEDGEMENTS

I would like to sincerely express my gratitude to my supervisor, Dr. Verónica Campanucci, who has given me such a unique and invaluable experience, which very much contributed in shaping my academic career in medicine. It was such a privilege working with a genuinely smart, kind and loving supervisor who supports everyone in the lab with her utmost sincerity, and at the same time challenges our critical thinking and reasoning abilities. To someone who always wishes for her students to succeed no matter what field of study they choose, and makes time out of her extremely busy days when we needed her help and advices. You have been a truly inspiring and admirable mentor.

To Zeinab, who has taught me most of the things I know in this lab. It would have been a considerably more difficult journey without your help and guidance. I will forever treasure your friendship and always look up to you as a big sister, whom we can always rely on whether be it from troubleshooting experiments to someone to give us life advices. It has been amazing learning from someone who has such a bright and fulfilling future ahead of them.

To everyone in the lab (Naseem, Wafa, Muniba, Nicolas and Jo), who has made every day in the lab enjoyable and exciting. It was always a pleasure learning new things about everyone's life, cultures and languages. Your passions for research and medicine have been contagious and motivating!

To my former and current committee members (Dr. John Howland, Dr. Thomas Fisher and Dr. Valerie Verge), thank you for keeping me on track and giving me constructive criticism and advices to better my research and academic career.

To the College of Medicine, for providing me with the opportunity to study and practice my research abilities in a scholarly and efficient manner.

Lastly, to my friends and family, most especially my parents, for continually giving me their unconditional support, love and encouragement every single day.

I will forever be thankful for the lessons I have learned in the past couple years in the Campanucci lab. The bonds that I have made with the people here are irreplaceable and will be held dearly in my heart. I wish you all the best in life and on your future endeavours, cheers!

TABLE OF CONTENTS

LIST OF TABLES

LIST OF FIGURES

LIST OF ABBREVIATIONS

AGEs	Advanced Glycation End-Products
ANOVA	Analysis of Variance
AP	Action Potential
C_m	Membrane Capacitance
CAP	Capsaicin
CNS	Central Nervous System
CTL	Control
DM	Diabetes Mellitus
DPN	Diabetic Peripheral Neuropathy
DSN	Diabetic Sensory Neuropathy
DRG	Dorsal Root Ganglion/Ganglia
E_{Na}	Reversal Potential for Sodium
ECF	Extracellular Fluid
EGTA	Ethylene Glycol-bis(2-aminoethylether)-N,N,N',N'-Tetraacetic Acid
G_{max}	Maximal Conductance
G_{Na}	Sodium Conductance
GLUT1	Glucose Transporter 1
GLUT2	Glucose Transporter 2
GLUT3	Glucose Transporter 3
HBSS	Hanks' Balanced Salt Solution
HEPES	N-2-Hydroxyethylpiperazine-N'-2-Ethanesulfonic Acid
HG	High Glucose
HRP	Horseradish Peroxidase
I_{Na}	Sodium Current
K^+	Potassium ion
lDRG	lumbar Dorsal Root Ganglion neurons
Lido	Lidocaine
MAPK	Mitogen-Activated Protein Kinase
MgATP	Adenosine 5'-Triphosphate Magnesium Salt

Na^+	Sodium Ion
Nav	Voltage-Gated Sodium
NFκB	Nuclear Factor kappa Beta
P0-P4	Postnatal day 0-4
P-loop	Pore loop
PKC	Protein Kinase C
RAGE	Receptor for Advanced Glycation End Products
S1-S6	Segments 1-6
SCG	Superior Cervical Ganglion
SDS-PAGE	Sodium Dodecyl Sulfate Polyacrylamide Gel Electrophoresis
SEM	Standard Error of Mean
STZ	Streptozotocin
TRPV1	Transient Receptor Potential for Vanilloid 1
TTX	Tetrodotoxin
TTX-R	Tetrodotoxin-sensitive
TTX-S	Tetrodotoxin-resistant
V_{half}	Membrane Potential for Half Maximal Activation
V_m	Membrane Potential
V_{rest}	Resting Membrane Potential
WT	Wild-Type

CHAPTER 1

INTRODUCTION

1.1. Diabetic Peripheral Neuropathy

Diabetes mellitus (DM) is a chronic metabolic disease characterized by deficiency in insulin production (Type 1) or resistance to insulin action (Type 2) (Kobayashi and Zochodne, 2018). Including both types 1 and 2, it was estimated that DM affected 415 million people worldwide in 2015, and its prevalence is predicted to rise to 642 million by 2040 (Ogurtsova et al., 2017). DM is linked to various forms of cellular and molecular disturbances in glucose and lipid metabolism, which lead to the activation of a host of complex biochemical pathways, making treatment highly challenging (Brownlee, 2001; Tomlinson and Gardiner, 2008). The hallmark feature of DM is hyperglycemia, or elevated levels of blood glucose, which is considered central to the pathophysiology of the disease (Tomlinson and Gardiner, 2008). Hyperglycemia leads to the development of a variety of complications, the most common being diabetic peripheral neuropathy (DPN) (Kobayashi and Zochodne, 2018). DPN affects approximately 50% of diabetic patients, depending on age, duration of diabetes and glycemic control (Said, 2007; Cheing, 2010; Callaghan et al., 2012). Moreover, up to 20% of diabetic patients can also experience the painful form of DPN (Callaghan et al., 2012). Therefore, as the prevalence of diabetic patients increases, the population of patients afflicted by DPN also increases.

Traditionally, DPN has been considered as the result of peripheral nerve damage after long-standing diabetes (Tesfaye et al., 2010). However, studies reporting the occurrence of DPN in prediabetic patients (Suo et al., 2016; Feldman et al., 2017; Wilson, 2017) and children with Type 1 DM (Louraki et al., 2012) are emerging. Moreover, it has been shown that patients with impaired glucose tolerance (but without overt diabetes) show early signs of neuropathy in skin biopsies, such as nerve fibre loss (Smith et al., 2001; Sumner et al., 2003). Ultimately, there is a need for a better understanding of the early mechanisms that initiate the pathogenesis of DPN before irreversible nerve damage ensues. DPN can affect all components of the peripheral nervous system, including sensory, motor and autonomic; however, DPN affecting sensory nerves is considered the most debilitating form (Tesfaye et al., 2010; Pop-Busui et al., 2017).

1.1.1. Diabetic Sensory Neuropathy (DSN)

Diabetic Sensory Neuropathy (DSN) is a subtype of DPN that affects the sensory nerves leading to sensory abnormalities. Forms of DSN can present with a wide spectrum of clinical symptoms from tingling, numbness, weakness, and sensory loss, to exacerbated pain perception (Callaghan et al., 2012; Kobayashi and Zochodne, 2018). Patients suffering from DSN can display one or more types of stimulus-evoked pain such as exacerbated responses to noxious (hyperalgesia) or innocuous (allodynia) sensory stimuli, and pain is often worse at night for patients (Hong et al., 2004; Tesfaye et al., 2010). The most common presentation for DSN is distal symmetrical polyneuropathy, in which sensory abnormalities most commonly manifest in a symmetrical "stocking-and-glove" distribution. Sensory abnormalities typically are experienced in the distal extremities (e.g., hands and feet) and progress proximally towards the torso over the course of diabetes (Callaghan et al., 2012). Consequently, diabetic patients are at a higher risk for developing foot ulcers, which can eventually contribute to lower limb amputations (Callaghan et al., 2012; Kobayashi and Zochodne, 2018). Ultimately, pathological damage to the peripheral nerves in DSN can be significantly debilitating, thereby resulting in considerable reduction in patient quality of life. Unfortunately, despite a strong relationship between blood glucose levels and neuropathy (The Diabetes Control and Complications Trial Research Group, 1993; Dyck et al., 1999), the underlying mechanisms contributing to the pathology of DSN are yet to be elucidated. Furthermore, while strict glycemic control and pain management are useful in DSN treatment, they are insufficient in arresting the progression of DSN. In addition, tight glycemic control has been shown to be more effective in preventing neuropathies in Type 1 DM, compared to Type 2 DM, potentially because of the differences in their underlying mechanisms (Vinik et al., 2000; Feldman et al., 2017). Therefore, unfortunately, there is no therapeutic strategy that has been successful in halting or reversing the progression of DSN (Boucek, 2006; Callaghan et al., 2012; Kobayashi and Zochodne, 2018).

1.1.2. Paradoxical Loss of Pain Perception and Pain Abnormalities in DSN

As mentioned above, DSN presents with a variety of sensory abnormalities, and the presence of both positive and negative symptoms in DSN is common. Patients can experience pain sensitivity

and paradoxical numbness at the same time (Callaghan et al., 2012). One of the biggest consequences of sensory loss in diabetes is “diabetic foot”. The diabetic foot results from lack of sensation making the feet susceptible to the recurring formations of unnoticed wounds or ulcers on a background of impaired wound healing. If left untreated, infections and gangrene can occur, leading to lower limb amputations (Jeffcoate and Harding, 2003). To prevent irreversible lower limb amputations, DSN patients are always advised to regularly check their feet for wounds and ulcers, and wear comfortable footwear (Pop-Bususi et al., 2017).

Along with the paradoxical loss of pain perception, patients also report painful sensations described as stabbing, electric or burning sensations (Kaur S. et al., 2011). Later on, as a result of long-standing diabetes, these incapacitating pain symptoms disappear, which unfortunately is a manifestation of the irreversible structural loss of sensory axons in the lower extremities (Boucek, 2006). During the onset of DSN, however, it is still under investigation if there are any early molecular and/or biochemical disturbances that contribute to the typical heterogeneous constellation of symptoms. The effects of hyperglycemia on neurons have been the focus of studies aiming at elucidating the pathogenesis of DSN.

1.1.3. Effect of Hyperglycemia on Neurons

Neurons are particularly vulnerable to the damages resulting from high glucose levels because neuronal glucose uptake is mostly dependent on the extracellular concentration of glucose (Patel et al., 1994; Tomlinson and Gardiner, 2008). Neurons are considered insulin-insensitive regarding glucose uptake, since the effects of insulin are markedly weaker in neurons than in other tissues. Glucose transporters 1 and 3 (GLUT1 and GLUT3) are uniporter transport proteins that mediate the facilitated transport of glucose across the plasma membrane of neurons, including those from the DRG (Rigon et al., 2013). Insulin, which has no effects on GLUT1 (Simpson et al., 2008), can indirectly regulate neuronal glucose uptake by promoting translocation of GLUT3 to a vesicles pool available to fuse with the plasma membrane. Fusion of GLUT3 to the plasma membrane is ultimately triggered by neuronal depolarization during periods of activity requiring the uptake of glucose (Uemura and Greenlee, 2006). Under diabetic

conditions, persistent hyperglycemia can result in up to a fourfold increase in glucose levels in neurons, making them more vulnerable to hyperglycemia-induced damage (Tomlinson and Gardiner, 2008). The hyperglycemia-induced neuronal insult is linked to a number of biochemical changes that ultimately lead to nerve damage. Proposed etiologies of DSN include increased polyol pathway flux leading to osmotic stress, increased hexosamine pathway flux and protein kinase C (PKC) activation resulting in altered gene expression and protein function, formation of advanced glycation end-products (AGEs), oxidative stress and inflammatory injury (for review, see: Brownlee, 2001; Tomlinson & Gardiner, 2008). AGEs are formed by the non-enzymatic glycation of proteins, nucleotides and lipids (Thornalley, 2002), which can lead to cross-linking of intra- and extracellular proteins, protein aggregation, and alterations in protein function (Vincent et al., 2007). Moreover, AGEs can bind to their receptor called RAGE (receptor for AGE), activating downstream signalling cascades leading to oxidative stress and inflammatory injury (Brownlee, 2001). In fact, RAGE signalling has been implicated in mechanisms of sensitization in sensory neurons under high glucose conditions (Lam et al., 2018). These complex pathological pathways contribute to the functional outcomes of DSN, such as reduced nerve conduction velocities, pain and impaired axonal regenerative capacity (Tomlinson and Gardiner, 2008).

1.2 The Sensory Nervous System and Pain Perception

The main role of primary sensory neurons is to convey sensory information from their innervated receptive fields to the central nervous system (CNS) for sensory integration. Sensory (afferent) nerves, along with motor (efferent) nerves, comprise the somatic nervous system, which is a branch of the peripheral nervous system. Humans have 31 pairs of spinal nerves categorized into regional segments as follows: 8 cervical, 12 thoracic, 5 lumbar, 5 sacral and 1 coccygeal (Krames, 2014). In the spinal cord, the dorsal horn receives sensory innervation from the dorsal root ganglion (DRG) via the neural foramina (Sapunar et al., 2012). The DRG contain cell bodies of sensory neurons that transduce sensory information from their peripheral terminals and transmit these signals to the dorsal horn of the spinal cord and eventually to the appropriate brain regions (Krames, 2014). As *Figure 1.1* illustrates, DRG neurons are pseudo-unipolar cells with a single process that bifurcates into a peripheral branch, which innervates target tissues and organs

(e.g. skin), and a central branch, which synapses onto second order sensory neurons in the dorsal horn of the spinal cord within laminae I and II in the case of C-fibers, and within laminae I and V for Aδ-fibres (Kandel et al., 2013). Pain, together with itch, temperature, and visceral information, is conveyed to the spinal cord by small-diameter myelinated and unmyelinated fibers. This information is conveyed across the midline within the spinal cord and transmitted to the brain stem and the thalamus in the contralateral anterolateral column, which then sends information to the somatosensory cortex (see *Fig. 1.1*) (Kandel et al., 2013). DRG neurons can span up to 1.5 meters in length, and are among the largest cells in the body (Hogan, 2010; Krames, 2014). Moreover, the DRGs are outside the blood-nerve barrier, and thus they are exposed to the circulating substances in the blood, including high levels of glucose in the case of DM (Sapunar et al., 2012).

Pain sensation is mediated by the small unmyelinated C-fibre neurons and the small to medium thinly-myelinated Aδ fibres from the DRGs; while Aβ fibres carry non-painful tactile sensory stimuli (Lai et al., 2004). Both small and large sensory fibres experience irreversible damage in DSN (Hong and Wiley, 2006; Jin and Park, 2017). In the late stages of diabetes, damage in these sensory neurons results in a "dying back" process of neurodegeneration, where distal axon terminals are more affected than axons in the proximal sites (Kobayashi and Zochodne, 2018). Yagihashi et al. (2011) proposed that DRG distal terminals are more vulnerable to the damages inflicted by diabetes because peripheral processes are of extended lengths, and thus nutrient and trophic support requires long transports from the cell body to the distal peripheral terminals. Over time, the largest and longest sensory processes innervating the hip, leg and feet display the most damage in DSN (Said, 2007; Kaur S. et al., 2011). Consequently, the present study included DRG neurons from the lumbar 1-5 regions of the spinal cord, which contain long sensory processes innervating the lower extremities.

DRG neurons express the transient receptor potential for vanilloid 1 (TRPV1) nonselective cation channel (Szallasi et al., 2007). This receptor is activated by a variety of ligands including capsaicin, which is the active ingredient found in chilli peppers (Szallasi et al., 2007). Activation of the TRPV1 channel causes a depolarization at the peripheral terminal, which if strong enough

can activate voltage-gated sodium (Nav) channels to fire an action potential (AP). The AP sends information from the peripheral terminal to the relay station in the spinal cord, from which the information is sent to the brain to be integrated as sensory perception (Boron and Boulpaep, 2017). Due to their central role in initiating AP firing, Nav channels have been implicated in the pathogenesis of DSN (Hirade et al., 1999; Craner et al., 2002; Hong et al., 2004; Hong and Wiley, 2006; Yang et al., 2016). Moreover, a strong correlation between Nav subunit expression and pain conditions has been shown in diabetic animal models and humans (Waxman et al., 1999; Benarroch, 2007; Tibbs et al., 2016). However, these studies mainly focused on the long-term effects of hyperglycemia, and the exact roles of Nav channels during the early stages of DSN are still under investigation.

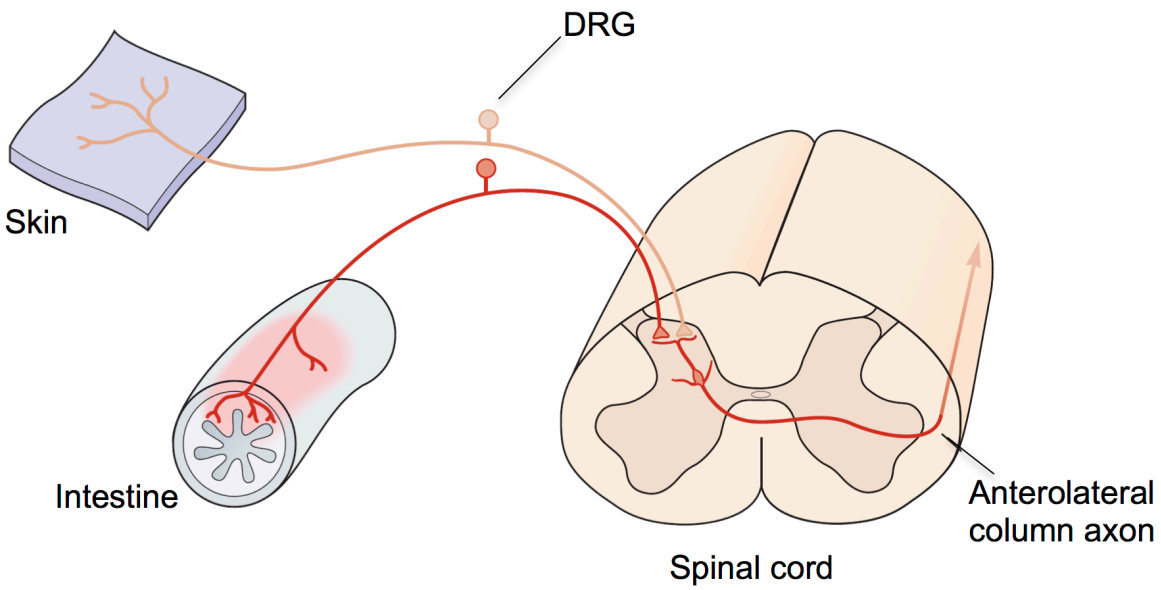

Figure 1.1. Diagram depicting a nociceptive pathway between the periphery and the spinal cord. Nociceptive fibers from pseudounipolar DRG neurons innervating the skin and viscera converge on projection neurons in the dorsal horn of the spinal cord. Sensory information is then carried by fibres of the anterolateral column pathway to the brain stem and the thalamus, and finally to the somatosensory cortex. **(Modified from Kandel et al., 2013)**

1.3. Voltage-Gated Sodium (Nav) Channels and AP Firing

In the peripheral terminals of DRG neurons, transducer receptors convert mechanical or chemical stimuli into an electrical signal called receptor potential. Receptor potentials are graded responses that if it causes a depolarization (membrane potential going in the positive direction) beyond a certain threshold voltage, an action potential response is initiated. An action potential (AP) is a regenerative all-or-none response of electrically excitable cells such as neurons (Boron and Boulpaep, 2017). It consists of three phases — a depolarizing phase, a repolarizing phase and a hyperpolarizing phase. The first phase of an AP is the depolarizing phase, wherein the membrane potential (V_m) of the cell becomes more positive. In DRG neurons, the V_m of a DRG neuron changes from a negative (usually around -60 mV) to a positive value until reaching the peak of the AP. The second phase involves the repolarizing of the membrane potential or returning to its resting value. The hyperpolarization phase occurs in APs of most excitable cells, where the V_m falls below the resting membrane potential (V_{rest}) before going back to V_{rest} (Boron and Boulpaep, 2017). Seminal work by Hodgkin and Huxley (1952) showed that APs occur due to the influx of Na^+ ions and efflux of K^+ ions (Hodgkin and Huxley, 1952) through voltage-gated channels (Boron and Boulpaep, 2017).

Voltage-gated sodium (Nav) channels are responsible for the depolarizing phase of APs. Nav channels are expressed throughout the nervous system, and they play critical roles in action potential generation and transmitting sensory information to the CNS (Catterall, 1992; Waxman et al., 1999). As *Figure 1.2* shows, Nav channels are composed of a large α-subunit, which associates with one or two auxiliary β-subunits (Lopez-Santiago et al., 2006; Benarroch, 2007). The α-subunit forms the ion-selective and voltage-sensitive pore of the channel (Lauria et al., 2014), while the β-subunit modulates Nav channel gating and membrane localization to distinct neuronal domains (Lopez-Santiago et al., 2006). The α-subunit is comprised of four homologous domains (domains I-IV), and each domain is made up of six α-helices called segments 1-6 (S1-S6) (Wang et al., 2011). The pore of the channel is composed of S5, S6 and a pore-loop (P-loop) that connects the two segments (De Lera Ruiz and Kraus, 2015). The voltage-sensing domain is formed by S1-S4, which regulates channel gating in response to membrane depolarization (De Lera Ruiz and Kraus, 2015). It has been proposed that membrane depolarization causes the S4

domain, which contains repetition of positively charged residues, to spiral outward towards the extracellular space, resulting in a conformational change that opens the pore of the channel (Wang et al., 2011). The latter results in activation of the channel, allowing sodium influx and further membrane depolarization to occur (Catterall, 1992). A key element of the Nav channel is the inactivation gate, which is formed by the intracellular loop between domains III and IV and acts as a hinged lid that plugs the pore of the channel in response to membrane depolarization (De Lera Ruiz and Kraus, 2015). Therefore, Nav channels exist in three functional states: closed, activated and inactivated (*Figure 1.3*) (Bagal et al., 2015). Nav channel activation causes depolarization, which in turn activates a larger population of Nav channels by a positive feedback mechanism. The latter is responsible for the rapidly rising phase of the AP. Following activation and while the cell is still depolarized, Nav channels enter an inactivated state, in which any further influx of Na^+ is prevented. The inactivation state is finally removed when V_m is restored (or by afterhyperpolarization), allowing the channels to return to the closed state and be ready for a new activation phase (Namadurai et al., 2015).

The α-subunit of Nav channels associates with one or two auxiliary β-subunits. β-subunits belong to the immunoglobulin superfamily of cell-adhesion molecules (Namadurai et al., 2015). To date, there are five β-subunits — β1, β1B, β2, β3 and β4. SCN1B-SCN4B encodes the four β-subunits and alternative splicing of the SCN1B gene results in the formation of the β1B subunit (Brackenbury and Isom, 2011; Namadurai et al., 2015). β1 and β3 noncovalently bind to the α-subunit, while β2 and β4 covalently attach to the α-subunit via disulfide bonds (Namadurai et al., 2015). β-subunits modulate gating, voltage-dependence and kinetics of Nav channels (Brackenbury and Isom, 2011). Among the different β subunits, Navβ2 have garnered much attention in pain research because SCN2B null mice exhibit altered pain responses (Pertin, 2005; Lopez-Santiago et al., 2006). During the biosynthesis of the Nav channels, Navβ2 associates with the α-subunit to enable plasma membrane insertion of the channel and thereby increases Nav current (Schmidt and Catterall, 1986). It has been proposed that the role of Navβ2 *in vivo* is to regulate tetrodotoxin-sensitive (TTX-S) Nav channels (Lopez-Santiago et al., 2006; Brackenbury and Isom, 2011). Lopez-Santiago and colleagues (2006) demonstrated that DRG neurons from $\beta2^{-/-}$ mice have significant reductions in TTX-S Nav currents compared to those from $\beta2^{+/+}$ mice and the observed decrease in TTX-S currents was supported by reductions in TTX-S Nav1.7

transcripts and protein levels. Furthermore, $\beta 2^{-/-}$ mice display increased sensitivity to noxious thermal stimuli (Lopez-Santiago et al., 2006), suggesting that Navβ2 may play key roles in the development of pain in neuropathic states.

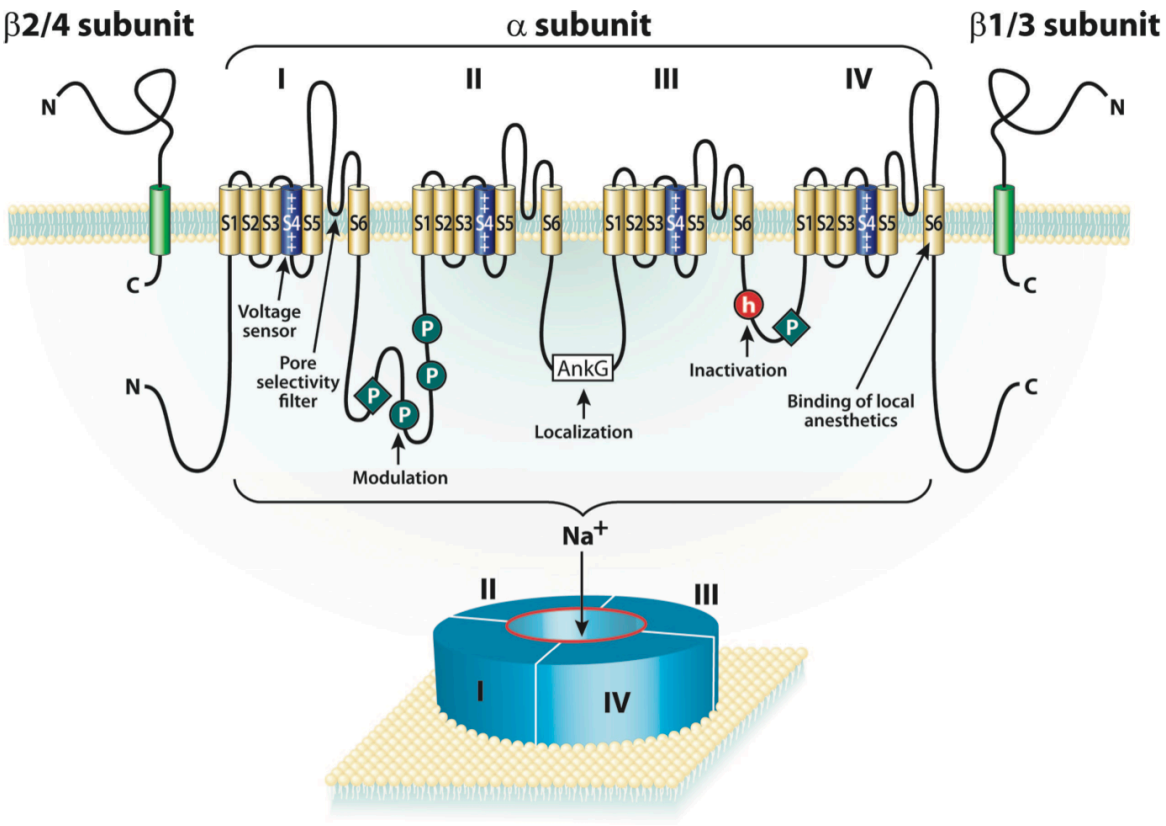

Figure 1.2. The primary structure of Nav channels is composed of a large α-subunit and one or two auxiliary β-subunits. The α-subunit is made up of four domains, and each domain is formed by six α-helical segments. The α-subunit folds to form the ion-selective and voltage-sensitive pore of the Nav channel. On the other hand, the β-subunit modulates channels gating and localization. **(Reproduced with permission from Benarroch, 2007)**

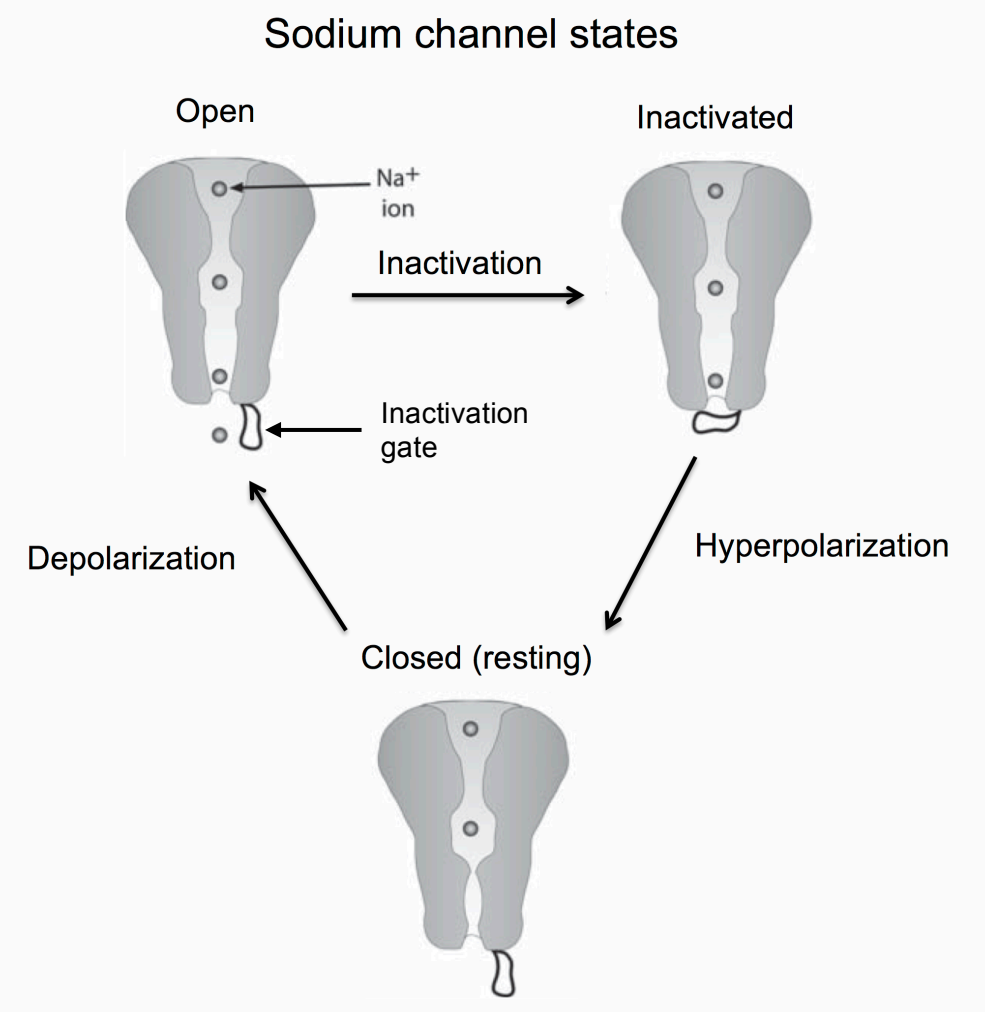

Figure 1.3. Nav channels cycle through three different states: closed, open and inactivated. A depolarization can activate Nav channels from the resting (closed) state into the open conformation to allow the influx of Na^+ ions. During depolarization, Nav channels enter an inactivated state where the inactivation gate acts as a hinged lid that plugs the pore of the channel. Then, a hyperpolarized membrane potential will return the Nav channel into its resting closed conformation, and the cycle will repeat for the next voltage stimulus. **(Modified from Bagal et al., 2015)**

1.3.1 Pharmacological Characterization of Nav Isoforms

There are nine Nav1 subtypes, Nav1.1 to Nav1.9, that have well-defined roles in neuronal physiology, and a novel family of Nav2 channels, whose function is still under investigation (De Lera Ruiz and Kraus, 2015). The different mammalian Nav isoforms display different kinetics and voltage dependencies (Benarroch, 2007; Waxman, 2012) and as a group, they are more than 50% homologous in their amino acid sequences (Goldin et al., 2000). The genes that encode different Nav isoforms are SCN1A (Nav1.1), SCN2A (Nav1.2), SCN3A (Nav1.3), SCN4A (Nav1.4), SCN5A (Nav1.5), SCN8A (Nav1.6), SCN9A (Nav1.7), SCN10A (Nav1.8) and SCN11A (Nav1.9) (De Lera Ruiz and Kraus, 2015). Nav isoforms can be pharmacologically classified according to their sensitivity to tetrodotoxin (TTX), which is a toxin isolated from animals such as the puffer fish. TTX blocks some Nav channels by binding to a neurotoxin receptor site on its outer pore (Chong and Ruben, 2008). Nav1.1, Nav1.2, Nav1.3, Nav1.4, Nav1.6 and Nav1.7 can be blocked by nanomolar concentrations of TTX, and thus are considered TTX-sensitive (TTX-S). On the other hand, Nav1.5, Nav1.8 and Nav1.9 are inhibited only by micromolar concentrations of TTX, and hence are viewed as TTX-resistant (TTX-R) (De Lera Ruiz and Kraus, 2015). In DRG neurons, TTX-S currents are mediated by Nav1.1, 1.3, 1.6 and 1.7, while TTX-R currents are carried by Nav1.8 and Nav1.9 (Benarroch, 2007). Most small DRG neurons have fast TTX-S Nav currents and a majority of them also co-express slow, TTX-R Nav currents (Parnham et al., 2005).

In addition, Nav channels are sensitive to local anaesthetics, such as lidocaine. Local anaesthetics work by blocking Nav channels in their inactivated state (De Lera Ruiz and Kraus, 2015). It is generally considered that lidocaine binds to the S6 segment of domain IV in the pore of the channel (Ragsdale et al., 1994). The mechanism of action of lidocaine makes it useful clinically as an antiarrhythmic and anaesthetic drug (De Lera Ruiz and Kraus, 2015). Moreover, lidocaine has been proposed as a treatment for neuropathic pain (Bach et al., 1990; Mao and Chen, 2000; Derry et al., 2014; Casale et al., 2017). Routes of administration include topical, oral and intravenous.

1.3.2. Nav Channels in Pain Abnormalities

Nociceptors express various Nav isoforms, such as Nav1.7, Nav1.8 and Nav1.9 (Rush et al., 2007). These isoforms have been implicated in the pathogenesis of multiple forms of neuropathic pain in humans and display distinct electrophysiological properties (Tibbs et al., 2016). First, Nav1.7 activates in response to small depolarizations, and serves to boost subthreshold stimuli (depolarizations that are below the voltage threshold to trigger an action potential response) to enable AP firing (Waxman, 2012). Nav1.7 is found in DRG and sympathetic neurons (Benarroch, 2007) and mutations in SCN9A gene have been linked to hereditary pain disorders such as primary erythromelalgia, paroxysmal extreme pain disorder and small fibre neuralgia (De Lera Ruiz and Kraus, 2015; Tibbs et al., 2016). Moreover, loss-of-function mutations in the SCN9A gene has been linked to congenital insensitivity to pain, a condition in which patients do not feel pain during situations such as childbirth, tooth extraction and broken bones (De Lera Ruiz and Kraus, 2015). Therefore, Nav1.7 plays key roles in the development of pain abnormalities and potentially during the onset of DSN.

Next, Nav1.8 carries majority of the inward current during the upstroke of the action potential and is specifically expressed in DRG neurons (Benarroch, 2007). Renganathan and colleagues (2001) demonstrated that Nav1.8$^{+/+}$ C-type DRG neurons were able to produce APs, while Nav1.8$^{-/-}$ DRG neurons only fire small graded potentials (Renganathan et al., 2017). Moreover, mutations in the SCN10A gene has been found in patients with painful small-fibre neuropathy (Faber et al., 2012). Nav1.7 and Nav1.8 have been proposed to work together during repetitive firing in DRG neurons (Lauria et al., 2014; De Lera Ruiz and Kraus, 2015). A study by Rush and colleagues (2006) demonstrated that one of the mutations (L858H) in the SCN9A gene identified in erythromelalgia has been shown to result in opposing phenotypes attributed to the presence or absence of the Nav1.8 channel. They showed that the L858H mutation in the SCN9A gene encoding for Nav1.7 results in a more depolarized V_{rest} in DRG neurons and sympathetic neurons from the superior cervical ganglion (SCG). However, this mutation resulted in hyperexcitability in DRG neurons and hypoexcitability in SCG neurons. These opposing effects have been associated with the presence or absence of the Nav1.8 channel in these cell types. DRG neurons have Nav1.8 and can sustain repetitive firing due to the depolarizations caused by Nav1.7, while SCG neurons lack the Nav1.8 channel and therefore the depolarizations caused by Nav1.7

inactivates other Nav channels (Nav1.3 and Nav1.6) ultimately leading to reduced excitability. (Rush et al., 2006; Benarroch, 2007). Moreover, diabetic patients have high levels of the reactive diacarbonyl methylglyoxal, which has been shown to induce post-translational modifications on Nav1.8 leading to increased excitability of nociceptive neurons and hyperalgesia (Bierhaus et al., 2012). Given its selective expression in DRG neurons and involvement in pain abnormalities, dysregulations in Nav1.8 may be involved in the development of symptoms in early DSN.

Nav1.9 produces a persistent current activated close to the resting membrane potential (Waxman, 2012). Mutations in the SCN11A gene has been linked to inflammation-induced hyperalgesia (Priest et al., 2005) and hyperexcitabilty of DRG neurons in familial episodic pain (Zhang et al., 2013). Lastly, Nav1.3 has garnered much attention in the field of neuropathic pain research. Nav1.3 displays an increase in expression levels following peripheral nerve injury and has been proposed to contribute to DRG neuron hyperexcitability (Waxman, 2012). Injured DRG neurons have been reported to exhibit an increase in TTX-S Nav currents and a reduction in TTX-R Nav currents and these changes have been attributed to an increase in expression levels of the TTX-S Nav1.3 and a simultaneous downregulation of the TTX-R Nav1.8 and Nav1.9 (Lai et al., 2004). Ultimately, Nav channels have been linked to pain abnormalities and may therefore mediate the positive and negative symptoms that occur in DSN.

1.4. Rationale and Hypothesis

A study by Lam et al. (2018) further supports increased sensory neuron excitability in DM even during short-term states. They reported that cultured DRG neurons maintained in high glucose for up to a week showed increased oxidative stress and a potentiation of capsaicin-evoked currents. Subsequent unpublished observations surprisingly revealed, however, that these sensory neurons are less excitable and fire fewer APs upon electrical stimulation. The latter contradicts the general consensus that DRG neurons in DM are hyperexcitable causing increased pain perception and suggests that hyperglycemia may modulate excitability differently over the course of the disease. Therefore, to better understand the molecular mechanisms underlying these contradictory findings, we hypothesized that short-term (10-14 days) exposure to high glucose affects the function of voltage-gated Na^+ (Nav) channels, which in turn affect the neuron's ability to generate APs.

The ultimate goal of this project was to elucidate the short-term effects of diabetes on the expression and function of Nav channels in DRG neurons. We studied Nav channel function in DRG neurons after exposure to a high glucose media. Next, to determine whether the changes conferred by glucose on Nav channels *in vitro* occurs during the very early stages of diabetes, we investigated Nav expression levels in intact DRG tissue from our diabetic mouse model. Our findings revealed that hyperglycemia modulates Nav channel expression and function in DRG neurons and that this modulation changes through the course of the disease. We hope this project will shed better light on the pathogenesis of DSN, and will aid in the development of therapeutics that could prevent the onslaught of irreversible DSN progression.

CHAPTER 2
MATERIALS AND METHODS

2.1 Primary Lumbar DRG Cultures. Primary DRG cultures were prepared from lumbar 1-5 [L1-L5] DRG neurons from C57BL/6 mouse pups between postnatal days 0-4 [P0-P4]. Briefly, DRGs were harvested under sterile conditions similar to the protocol for superior cervical ganglion neurons (Campanucci et al., 2008). The DRG neurons were utilized because they contain long processes, which display the most damage in DSN (Said, 2007). The removed ganglia were then dissociated at 37°C in Hanks' balanced salt solution (HBSS) containing trypsin (1 mg/mL; Worthington, Freehold, NJ) and buffered with HEPES (N-2-hydroxyethylpiperazine-N'-2-ethanesulfonic acid) for 45-60 minutes. Afterwards, the ganglia were triturated 50-100 times using fire-polished pipettes until dissociated. The resulting cell suspension was washed twice using serum-containing media to inactivate trypsin, then plated on laminin-coated glass bottom Petri dishes (Corning 35 mm) made in-house. The DRG neurons were maintained in a growth media made from Leibovitz's L-15 medium supplemented with vitamins, cofactors, penicillin-streptomycin, 5 mM glucose, 5% rat serum, and NGF (nerve growth factor, 10 ng/mL). The primary DRG cultures were kept at 37°C in a 95% air-5% CO_2 atmosphere, and fed every 4-5 days. To eliminate non-neuronal cells, cultures were treated with cytosine arabinoside (10 μM; Sigma, St. Louis, MO) containing media from days 2 to 4 after culturing. Cultures were maintained in either a control (5 mM; CTL) or high glucose (25 mM; HG) media for an additional 10-14 days before any whole-cell patch clamp experiments were performed.

2.2 Animals. One-month-old male C57BL/6 mice were intraperitoneally injected with streptozotocin (STZ; 50 mg/kg) or with citrate buffer (control; CTL; pH=4.5) for 3 consecutive days. STZ is an antibiotic that destroys the insulin-producing β cells of the pancreas (Deeds et al., 2011). STZ is taken up by β cells via the glucose transporter 2 (GLUT2), and causes DNA alkylation leading to cell death (Gleichmann and Wang, 1998; Szkudelski, 2001; Deeds et al., 2011). After one or three month(s), intact L1-5 DRG tissues were collected from control and diabetic animals. Diabetes was defined as a final blood glucose level of 15 mM or greater. Initial measurements of body weight and blood glucose were taken at day 1 of STZ injections, while final measurements were taken on the day of euthanasia and sample collection. Control animals

with blood glucose levels above 10.5 mM during sample collection were considered prediabetic and were excluded from this study (Campanucci et al., 2010). Animals were provided access to normal rodent chow *ad libitum*.

2.3 Whole-Cell Patch Clamp Electrophysiology. Primary DRG cultures maintained in either control (5 mM) or high glucose (25 mM) conditions were utilized in whole-cell patch-clamp electrophysiological experiments. Patch pipettes were made from borosilicate glass (World Precision Instruments, Sarasota, FL, USA) using a vertical puller (PC 10; Narishige Scientific Instrument Lab., Tokyo, Japan), and had a resistance of 3–8 MΩ when filled with intracellular recording solution. Recording electrodes were filled with the following intracellular solution (in mM): 60 $KC_2H_3O_2$, 70 KF, 5 NaCl, 1 $MgCl_2$, 1 $CaCl_2$, 10 HEPES (N-2-hydroxyethylpiperazine-N'-2-ethanesulfonic acid), 10 EGTA (ethylene glycol-bis(2-aminoethylether)-N,N,N',N'-tetraacetic acid) and 2 Mg-ATP (adenosine 5'-triphosphate magnesium salt), and pH was adjusted to 7.2 with KOH (all from Sigma–Aldrich). Cultured neurons were perfused continuously at 2 mL/min with extracellular fluid (ECF) consisting of (in mM): 140 NaCl, 5.4 KCl, 0.33 NaH_2PO_4, 0.44 KH_2PO_4, 2.8 $CaCl_2$, 1 $MgCl_2$, 10 HEPES, 5.0 glucose (all from Sigma-Aldrich); pH was adjusted to 7.4 with NaOH. Whole-cell currents or membrane potentials were recorded at room temperature with the aid of an Axopatch 200B amplifier (Molecular Devices, Palo Alto, CA, USA) equipped with a 1 GΩ headstage feedback resistor and a Digidata 1440A (Molecular Devices) and stored on a personal computer. Voltage- and current-clamp protocols, data acquisition, and analysis were performed using pCLAMP 10 software (Molecular Devices) and OriginPro 9.0 (OriginLab Corporation, Northampton, MA, USA). Patched DRG neurons were allowed to stabilize for 5 minutes before data collection. For voltage-clamp recordings, a hyperpolarizing prepulse of -120 mV was applied from a holding potential of -60 mV. Then, a step protocol from -80 mV to +30 mV at 10mV increments was applied to generate inward currents. For current-clamp recordings, action potentials (AP) were generated by the injection of depolarizing current steps (100 pA intervals for 500 ms). In both configurations, additional perfusions with added 1 μM tetrodotoxin (TTX; Alomone Labs), and 1 μM TTX + 100 μM lidocaine (Sigma-Aldrich) were used to better isolate sodium currents.

2.4 Whole-Cell Currents Analysis. The TTX-sensitive (TTX-S) component of the whole-cell inward currents was isolated by subtracting recordings obtained with TTX from those without (control); while TTX-resistant (TTX-R) currents were isolated by subtracting recordings with TTX + lidocaine from those done with TTX alone. Conductance values were obtained by the following formula:

$$G_{Na} = \frac{I_{Na}}{V_m - E_{Na}} \quad \text{.....(2.1)}$$

Where G_{Na} is the conductance for sodium ions (Na^+), I_{Na} is the peak current at a specific test pulse, V_m is the voltage step, and E_{Na} is the reversal potential for Na^+. E_{Na} was calculated to be +84.3 mV in the experiment setup using the Nernst equation. G_{Na} was normalized to maximum conductance (G_{max}). Steady-state activation curves were acquired by fitting normalized conductance (G_{Na}/G_{max}) values in the Boltzmann equation:

$$y = \frac{(x - E_{Na}) * G_{max}}{1 + e^{(x - V_{half})/dx}} \quad \text{.....(2.2)}$$

Where, E_{Na} is the reversal potential for Na^+, G_{max} is the maximal conductance, and V_{half} is the membrane potential at half-maximal activation.

2.5 Western Blotting. DRG tissue samples were lysed using CelLytic™ MT Cell Lysis Reagent (Sigma, St. Louis, MO) with 1x Halt™ Protease and Phosphatase Inhibitor Cocktail, EDTA-free (ThermoFisher Scientific). Equal amounts of proteins were loaded and separated using a 12% SDS-PAGE (sodium dodecyl sulfate polyacrylamide gel electrophoresis) gel. The gel was then electrotransferred onto a nitrocellulose membrane and probed with rabbit anti-mouse Nav1.3 (1:500, Alomone Labs), rabbit anti-mouse Nav1.6 (1:500; Alomone Labs), rabbit anti-mouse Nav1.7 (1:500, Alomone Labs), rabbit anti-mouse Nav1.8 (1:500, Alomone Labs), rabbit anti-mouse Nav1.9 (1:500, Alomone Labs), rabbit anti-mouse Navβ2 (1:500, Alomone Labs), or mouse anti-β-actin (1:2000, Abcam) primary antibodies. Afterwards, the blots were probed using the appropriate horseradish peroxidase (HRP)-conjugated anti-rabbit/mouse secondary antibodies (1:5000; Bio-Rad Laboratories). Protein signals were visualized using enhanced chemiluminescence reagents (Bio-Rad) and quantified by densitometry using ImageJ software

(NIH). All Nav protein signals were normalized to those of β-actin, and expressed as percent of control.

2.6 Statistical Analysis. All data are reported as mean ± standard error of mean (SEM). A two-way analysis of variance (ANOVA) followed by a Tukey's *post hoc* test was used to analyze voltage-clamp (maximum peak current densities) and current-clamp (action potential frequency) data. For body weight and blood glucose measurements, we performed a repeated measures two-way ANOVA followed by a Sidak's *post hoc* analysis. A Student's *t*-test or Mann-Whitney test was employed to analyze signal intensities between groups in western blotting, and to compare parameters in activation curves. In all cases, data with p values less than or equal to 0.05 were considered statistically significant. All statistical analyses were performed using InStat 3.0 or Prism 8 (both from GraphPad Software Inc., La Jolla, CA, USA).

CHAPTER 3
RESULTS

3.1 Short-term exposure of cultured DRG neurons to high glucose decreases neuronal excitability

The passive membrane properties of all cells that I patch-clamped are reported in *Table 3.1*. There were no significant differences ($p>0.05$) found in membrane capacitance (C_m) expressed in picofarads (pF), and resting membrane potential (V_{rest}) expressed in millivolts (mV) between the control (CTL; 5 mM glucose) and high glucose (HG; 25 mM glucose) groups.

As a measure of neuronal excitability, current-clamp recordings were utilized to study action potential (AP) firing frequency in cultured DRG neurons. APs were generated by the injection of 100 pA depolarizing current for increments of 500 ms. APs were compared between CTL and HG groups using three perfusing solutions: no blockers, 1 μM tetrodotoxin (TTX), and 1 μM tetrodotoxin + 100 μM lidocaine (TTX + Lido). Exposure to HG for 10-14 days reduced evoked AP firing, with respect to CTL (*Figure 3.1*) and this reduction was statistically significant at a current injection of 500 pA ($p<0.001$) (*Figure 3.1C*). At 500 pA, the AP frequency (s^{-1}) for the CTL and HG groups were 12.26 ± 2.58 and 3.88 ± 0.71, respectively. There were no significant differences ($p>0.05$) between the CTL and HG groups when TTX or TTX + Lido was added to the perfusing bath solution. The AP frequency for those groups are 6.69 ± 2.04 for CTL TTX, 2.42 ± 0.19 for HG TTX, 2.00 ± 0.63 for CTL TTX + Lido, and 1.54 ± 0.24 for HG TTX + Lido.

Table 3.1. Passive membrane properties of DRG neurons in control and high glucose. There were no significant differences between the membrane capacitance (C_m; pF) and the resting membrane potential (V_{rest}; mV) between the control (CTL) and high glucose (HG) groups. Analyses were performed using Student's *t*-tests. CTL: n=15, HG: n=18.

	C_m (pF)	**V_{rest} (mV)**
CTL (n=15)	17.37 ± 1.17	-51.17 ± 1.31
HG (n=18)	18.25 ± 1.02	-54.11 ± 1.66

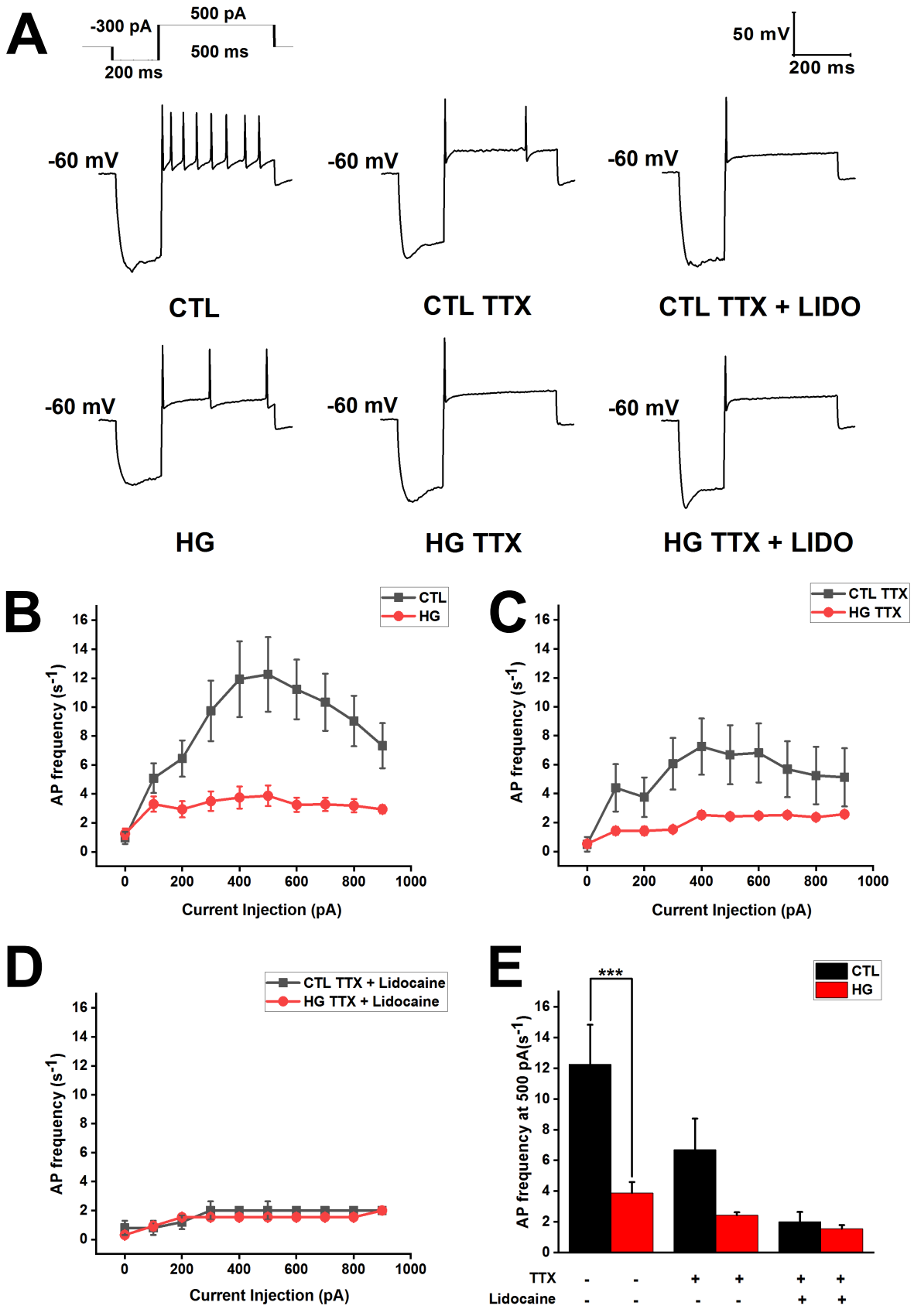
A
-300 pA
500 pA
500 ms
200 ms
50 mV
200 ms
-60 mV
CTL
CTL TTX
CTL TTX + LIDO
HG
HG TTX
HG TTX + LIDO
B
CTL
HG
AP frequency (s-1)
Current Injection (pA)
C
CTL TTX
HG TTX
D
CTL TTX + Lidocaine
HG TTX + Lidocaine
E
***
AP frequency at 500 pA(s-1)
TTX
Lidocaine

Figure 3.1. Sensory neurons from the DRG fire fewer action potentials (APs) after short-term exposure (10-14 days) to high glucose. **A.** Representative current-clamp traces under control (CTL) and high glucose (HG) conditions, recorded with normal bathing solution, with tetrodotoxin (TTX), or with TTX + lidocaine (TTX + Lido). Recordings were generated using a current-clamp protocol (inset) from a holding potential of -60 mV. **B-D.** Line graphs demonstrate AP frequency (s^{-1}) at different current step injections (pA) with no blockers (B), TTX (C), and TTX + Lido (D). **E.** Analysis at 500 pA indicates a significant reduction in AP frequency between CTL and HG conditions. Statistical analysis performed using a two-way ANOVA followed by a Tukey's *post hoc* test. CTL n=27, HG n=32, CTL TTX n=16, HG TTX n=19, CTL TTX + LIDO n=5, HG TTX + LIDO n=13. ***indicates $p<0.001$.

3.2 Short-term exposure to high glucose decreases voltage-gated Na^+ currents in DRG neurons

To better understand the possible role of Nav channels in the decreased AP firing frequency in HG conditions, we studied voltage-gated Na^+ currents in CTL and HG conditions. We used voltage-clamp electrophysiology, at a holding potential of -60 mV followed by a hyperpolarizing prepulse (-120 mV) to remove Nav inactivation and subsequent step voltages (-80 mV to +30 mV at 10 mV increments), to generate inward current including Nav currents. HG (10-14 days) caused a significant decrease in the peak current density with respect to control, in the three experimental conditions: CTL and HG (p<0.01), CTL TTX and HG TTX (p<0.001), and CTL TTX + Lido and HG TTX + Lido (p<0.05) (*Figure 3.2*). The maximum peak current densities (pA/pF) for each group are -165.27 ± 9.65 for CTL, -112.02 ± 11.96 for HG, -132.40 ± 10.22 for CTL TTX, -65.18 ± 10.97 for HG TTX, -83.31 ± 8.22 for CTL TTX + Lido, and -35.20 ± 8.28 for HG TTX + Lido.

To determine whether the effects of short-term exposure to high glucose were mediated by changes in the activation kinetics of Nav channels, we generated the activation curves shown in *Figure 3.3*. There were no significant differences in the membrane potential for half-maximal activation (V_{half}) between CTL (-28.48 ± 1.74 mV) and HG (-31.77 ± 12.68 mV) groups.

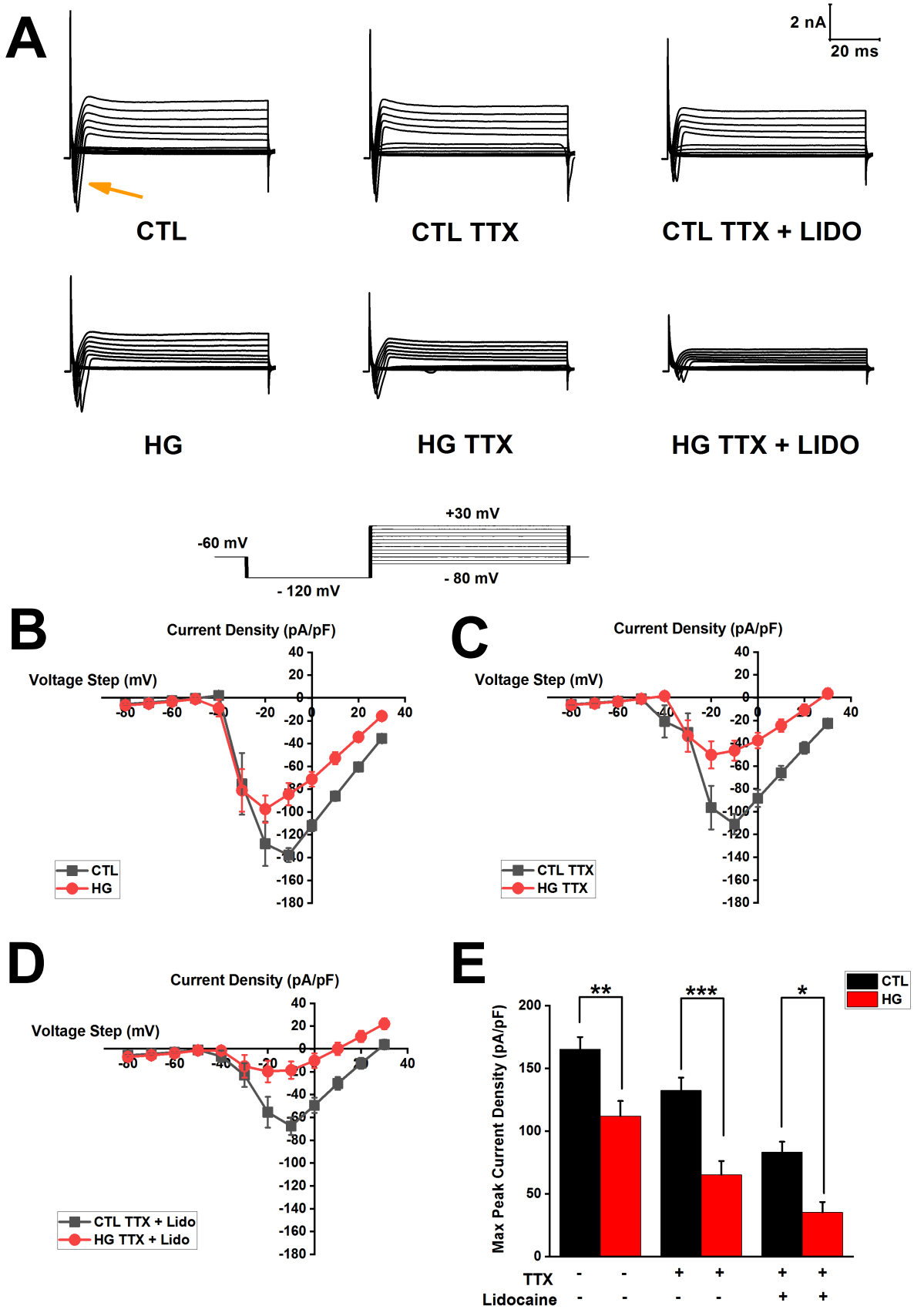
A
2 nA
20 ms
CTL
CTL TTX
CTL TTX + LIDO
HG
HG TTX
HG TTX + LIDO
+30 mV
-60 mV
- 120 mV
- 80 mV
B
Current Density (pA/pF)
Voltage Step (mV)
CTL
HG
C
Current Density (pA/pF)
Voltage Step (mV)
CTL TTX
HG TTX
D
Current Density (pA/pF)
Voltage Step (mV)
CTL TTX + Lido
HG TTX + Lido
E
CTL
HG
Max Peak Current Density (pA/pF)
**
***
*
TTX
Lidocaine

Figure 3.2. Sensory neurons from the DRG generate less inward currents in HG. **A.** Representative voltage-clamp traces in CTL (top) and HG (middle) conditions generated by the protocol displayed at the bottom. The orange arrow points at a representative example of inward currents. **B-D.** Line graphs display the mean ± SEM of the peak current densities (pA/pF) plotted against voltage step (mV) with no blockers (B), TTX (C) and TTX + Lidocaine (D). **E.** The maximum peak current densities (pA/pF) show significant reductions between CTL and HG, CTL TTX and HG TTX, and CTL TTX + Lido and HG TTX + Lido. Note, maximum peak current densities were reported as positive values for easier visualization in E. Statistical analysis was performed using two-way ANOVA followed by Tukey's *post hoc* test. CTL n=15, HG n=18, CTL TTX n=14, HG TTX n=18, CTL TTX + Lido n=14, HG TTX + Lido n=16. *indicates $p<0.05$, **indicates $p<0.01$, ***indicates $p<0.001$.

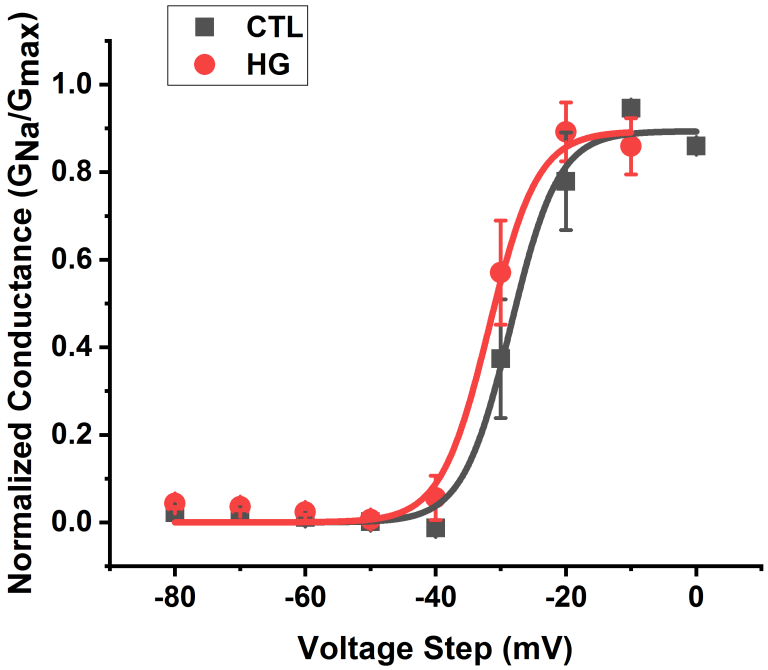

Figure 3.3. Activation curves for voltage-gated inward currents in DRG neurons. There was no significant difference in activation parameters between CTL and HG. Current-voltage curves from *Figure 3.2B* were converted to conductance-voltage relationships and fitted into a Boltzmann equation as described in *Materials and Methods*. Statistical analysis performed by Student's *t*-test. CTL n=15, HG n=18.

3.3 Short-term diabetes decreases the expression levels of TTX-S Nav subunits

To determine whether the observed effects of high glucose on Nav currents *in vitro* were reflected by changes in the expression levels of Nav subunits in the DRG *in vivo*, we employed a mouse model of diabetes. In the present study, Nav expression levels were analyzed at one month, as a short-term time point, and at three months, as a long-term time point, after STZ-induction of diabetes.

The body weights and blood glucose levels of the mice included in the one-month group are reported in *Figure 3.4A-B*. *Figure 3.4A* displays the mouse body weights, which were 23.31 ± 0.53 g for the initial weight of CTL mice, 20.50 ± 0.32 g for the initial weight of STZ mice, 24.87 ± 0.49 g for the final weight of CTL mice, and 21.04 ± 0.46 g for the final weight of STZ mice. The initial and final body weights of the CTL group were statistically different from one another ($p<0.01$). We also found significant differences between the initial body weights of the CTL vs STZ ($p<0.001$) and between the final body weights of CTL vs STZ ($p<0.001$) groups. *Figure 3.4B* displays the blood glucose levels of the mice included in the one-month group, which were 9.14 ± 0.42 mM for the initial of CTL, 9.87 ± 0.33 mM for the initial of STZ, 8.46 ± 0.32 mM for the final of CTL, and 31.73 ± 0.89 mM for the final of the STZ group. The final blood glucose of the STZ group is significantly higher than those of CTL ($p<0.001$) and the initial levels of the STZ group ($p<0.001$), confirmed diabetic conditions in these animals.

At one month after STZ-induced diabetes, there were significant downregulations in the expression levels of different Nav subunits. Reported as percentages of control (%), the Nav protein expression levels were 74.05 ± 2.30 for Nav1.3, 70.93 ± 5.32 for Nav1.6, 77.23 ± 1.87 for Nav1.7, 93.35 ± 7.51 for Nav1.8, 89.06 ± 8.33 for Nav1.9, and 67.91 ± 7.02 for Navβ2 (*Figure 3.4C-D*). There were significant reductions for Nav1.3, Nav1.6, Nav1.7 and Navβ2. Interestingly, all three Nav α-subunit isoforms are TTX-S.

Next, we used a group of animals that had been STZ-induced diabetic for 3 months. Body weights and blood glucose levels are illustrated in *Figure 3.5A-B*. The initial body weights were 20.16 ± 0.64 g for CTL and 20.89 ± 0.56 g for STZ and the final body weights were 30.25 ± 0.80 g for CTL and 25.44 ± 1.33 g for STZ. The final body weights for both groups were significantly

different from their corresponding initial measurements (p<0.001 for CTL and p<0.01 for STZ) and the final body weight of the STZ group is significantly lower (p<0.001) than those of CTL. The initial blood glucose levels of the three-month group were 11.55 ± 0.64 mM for CTL and 12.80 ± 0.36 mM for STZ and the final blood glucose levels were 8.78 ± 0.28 mM for CTL and 31.60 ± 1.16 mM for STZ. The final blood glucose measurements of both groups were significantly different from their corresponding initial values (p<0.01 for CTL and p<0.001 for STZ). In addition, the final blood glucose level of the STZ group was significantly higher (p<0.001) from those of the CTL group, which again confirms diabetic states.

Biochemical analysis of lumbar DRG samples collected from animals made diabetic by STZ for three months show a striking difference from the Nav subunit expression profile observed at one-month diabetes (*Figure 3.5D*). At three months, we found a significant increase in the expression levels of the TTX-S Nav1.7. Expressed as a percentage of CTL, the protein expression level of Nav1.7 became 180.97 ± 6.35% three months after the induction of diabetes, while there were no significant changes in the rest of the Nav subunits. For the rest of the subunits, their protein expression levels in percent (%) were as follows: 102.76 ± 9.37 for Nav1.3, 117.35 ± 9.16 for Nav1.6, 191.95 ± 19.13 for Nav1.8 (p=0.057), 181.99 ± 34.84 for Nav1.9 (p=0.200), and 123.36 ± 17.35 for Navβ2.

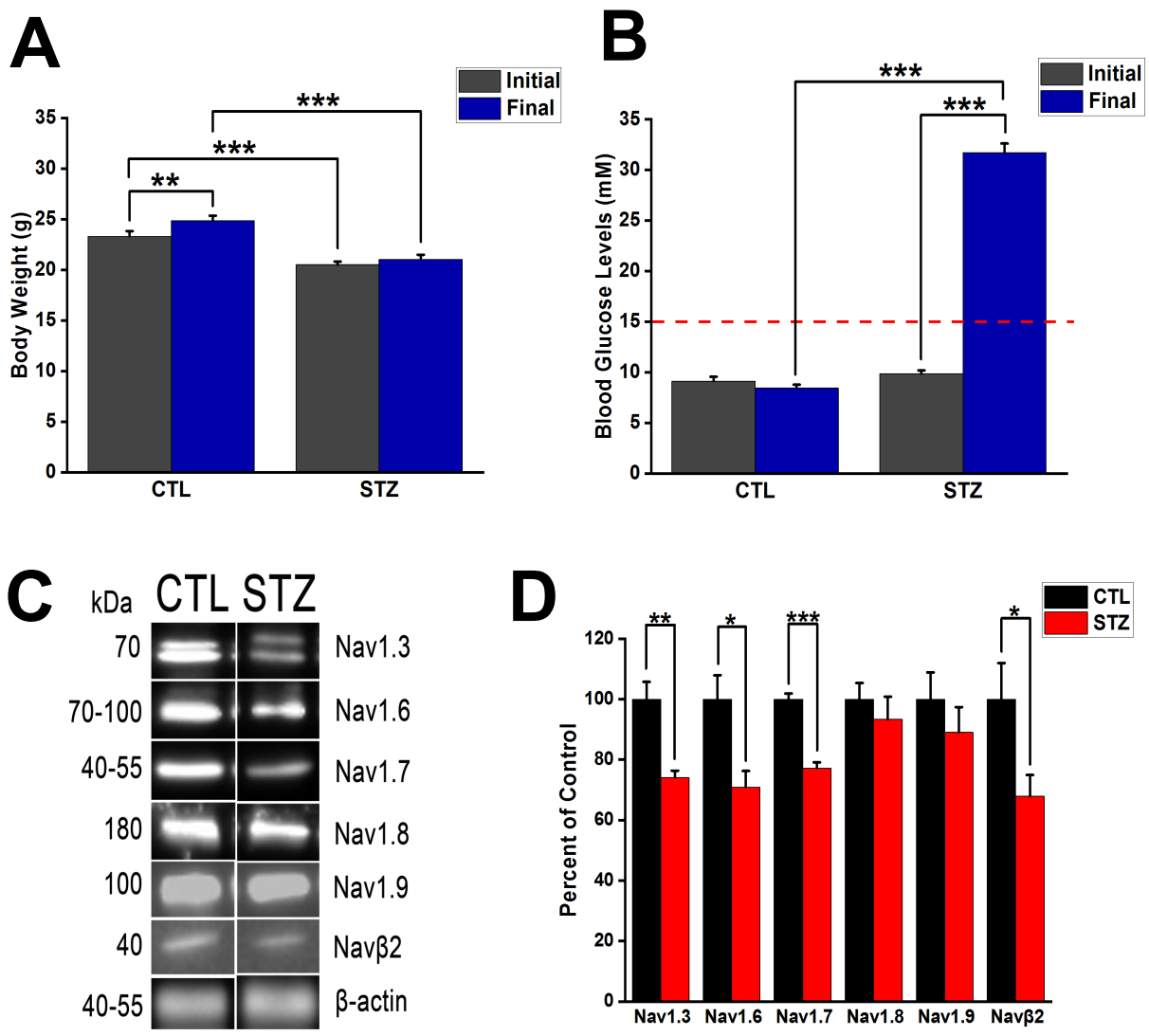

Figure 3.4. Initial and final body weights (**A**) and blood glucose levels (**B**) of the animals used for the one-month STZ-diabetic group. Significant differences were found in the initial and the final body weights between CTL and STZ groups, and between the initial and final values in the CTL group. In addition, the final blood glucose level of the STZ group was statistically higher than the initial of the STZ and the final of the CTL group. **C.** Representative immunoblots showing detection levels of various Nav channel subunits from intact DRG tissues collected from CTL and STZ-diabetic mice at one month after induction of diabetes. **D.** Bar graphs summarize the quantification of protein levels normalized to β-actin and expressed as percentages of control. There were statistically significant reductions in the expression levels of Nav1.3, Nav1.6, Nav1.7 and Navβ2. All three α-subunits are TTX-S. Statistical analyses were done by two-way repeated measures ANOVAs followed by Sidak's *post* hoc tests for A and B (CTL n=31, STZ n=42) and Student's *t*-tests for D (n=5 per group). *, indicates $p<0.05$; **, indicates $p<0.01$; ***, indicates $p<0.001$.

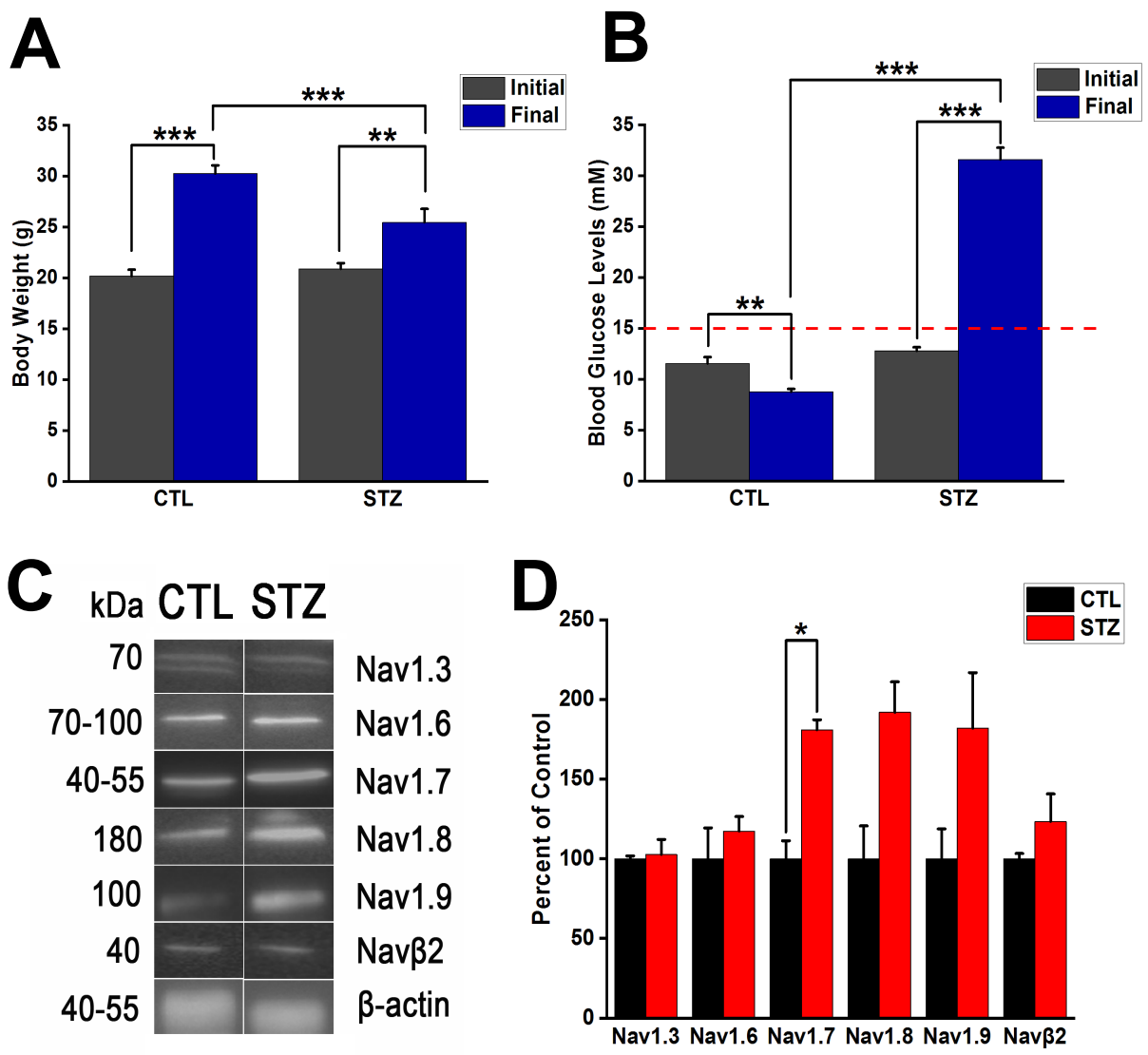

Figure 3.5. Initial and final body weights (**A**) and blood glucose levels (**B**) of CTL and STZ mice of the three-month STZ-diabetic group. The final weights of the CTL and STZ groups are statistically different from their own initial values and the STZ final weight is also statistically different from the CTL final weight. The final blood glucose levels of the CTL and STZ groups were statistically significant from their corresponding initial measurements and the STZ final blood glucose level was statistically higher than the CTL and STZ initial values. **C.** Representative immunoblots showing detection levels of various Nav channel subunits from intact DRG tissues collected from CTL and STZ-diabetic mice at three months after induction of STZ-diabetes. **D.** Bar graphs summarize the quantification of protein levels normalized to β-actin, and expressed as percentages of control. There was a significant increase in the expression level of the TTX-S Nav1.7 subunit. Statistical analyses were performed by two-way repeated measures ANOVA followed by Sidak's *post hoc* tests for A and B (CTL n=16, STZ n=9), and non-parametric Mann-Whitney test for D (n=3 per group for Nav1.3, and n=4 per group for the rest of the subunits). *, indicates $p<0.05$; **, indicates $p<0.01$; ***, indicates $p<0.001$.

CHAPTER 4
DISCUSSION AND CONCLUSION

4.1 Effect of High Glucose and Short-Term Diabetes on DRG Neurons

Diabetic peripheral neuropathy (DPN) manifests through many sensory abnormalities that at advanced stages of the disease are accompanied by structural abnormalities in affected sensory nerves. Although DPN has been traditionally considered as resulting from long-standing diabetes, many studies demonstrate the prevalence of DPN in disorders with a very different and shorter time course, such as in prediabetic patients (Stino and Smith, 2017; Wilson, 2017) or in children diagnosed with Type 1 diabetes (Louraki et al., 2012). In addition, further challenging the traditionally-accepted view, research on DRG neurons *in vitro* show that high glucose can have detrimental effects on sensory neurons independent from glia- or blood vessels-mediated effects, and that sensory neuron abnormalities can develop in a matter of 1-2 weeks (Russell et al., 1999; Lam et al., 2018).

Therefore, a better understanding of the molecular, biochemical and functional mechanisms that contribute to the pathology of DPN is required. In this study, we demonstrate that short-term exposure (10-14 days) of DRG neurons to high glucose alters the function of Nav channels. Contrasting with the known effect of hyperglycemia on DRG neurons, which leads to increased sensory responses (e.g. to capsaicin) (Pabbidi et al., 2008; Lam et al., 2018), our study showed that 1-2 weeks of high glucose treatment caused a decrease in sensory neuron responses, such as reduction in the generation of action potentials. Consistent with this finding, we observed reduced inward currents, without alteration in activation kinetics.

It is important to point out that in the presence of TTX alone, high glucose was still effective in reducing the inward currents compared to CTL (i.e. CTL TTX vs HG TTX). This reduction could be attributed to failure in total block of TTX-S currents in CTL and/or HG conditions, or to another type of inward current affected by HG. The latter is supported by preliminary data (unpublished observations) from our own laboratory indicating that T-type Ca^{2+} currents are significantly reduced by the high glucose treatment. Further research is required to understand the

combined effect of high glucose and short-term diabetes on Nav and T-type Ca^{2+} currents, and how this impacts cell excitability.

Our western blotting experiments support the idea that short-term diabetes and high glucose impact TTX-S Nav channels. In the DRG of animals one month after the induction of diabetes, we observed a reduction in the expression levels of the TTX-S subunits of Nav channels. The observed decrease in inward currents contrast with previous reports on the function of Nav channels in the DRG of diabetic animal models (Hirade et al., 1999; Hong et al., 2004; Kharatmal et al., 2015). This opposite effect could be attributed at least in part to the age of our experimental animals, which were neonates for our *in vitro* model. A study by Kharatmal and colleagues (2015) demonstrated increased TTX-R current densities in DRG neurons exposed to high glucose conditions of 30 mM for 24 hours. This study was performed on 3-4 month old rats, while our experiments utilized DRG neurons from mice pups 0-4 days postnatally. Despite the contradictory findings, both studies support the notion that short-term exposure to high glucose exerts functional effects on Nav channels independent of the structural and vascular changes associated with long-term diabetes (Bellini et al., 2017). In addition, studies from animal models of STZ-diabetes reported increases in Nav currents (Hirade et al., 1999; Hong et al., 2004). These studies were performed on STZ-induced diabetic rats, which ranged from ages of 4 weeks to 8 months old, while our studies were performed on neonatal mice for *in vitro* experiments. Moreover, their electrophysiological recordings were performed 2-7 hours after cell preparation, while our primary DRG cultures were allowed 5 days to recover before we exposed them to high glucose conditions. Considering that the trauma of axotomy during neuronal isolation is known to induce oxidative stress, which can trigger apoptotic signalling (Sayir et al., 2013), the contrasting findings could be potentially based on the health of the culture neurons. In a recent publication from our team (Lam et al., 2018), we addressed this point by demonstrating that cultured DRG neurons exposed to high glucose were under oxidative stress, but not in an apoptotic state.

Thus, our study revealed that short-term exposure (10-14 days) to high glucose decreases DRG neuron excitability and we provided evidence for possible early functional changes that occur in DPN, potentially when patients are still asymptomatic. Considering that variability in the species and experimental designs between our study and previously reports may be contributing to the

differences in findings, it will be relevant to investigate electrophysiological properties of DRG neurons from our adult STZ-diabetic animals.

To validate our *in vitro* findings, we employed a diabetic mouse model. We observed some unpredicted effects on body weight and blood glucose levels that are worth further considering. First, we observed a significant difference between the initial body weights of the CTL and STZ mice in our one-month group. We can only attribute that difference to chance during animal selection for the experimental groups, wherein the STZ group were a batch of smaller animals compared to the CTL group. Second, in both the one- and three-month groups, the final body weight of the STZ group was significantly lower than those of CTL mice, which is consistent with previous reports of the link between STZ-induced diabetes and weight loss due to factors such as an increase in urine output (Graham et al., 2011), which possibly contributed to the decrease in the final weight of the STZ group. Third, we observed that the initial blood glucose levels of both groups were higher than expected for young control mice (10.6-14.9 mM). This effect could be explained by the effect of the anesthetic isoflurane, which is known to increase blood glucose levels (Windeløv, Pedersen, & Holst, 2016). Accordingly, once isoflurane was avoided before euthanasia, the final blood glucose levels of CTL animals were within the normal range (i.e. 10.5 mM or lower).

4.2 Changes in Expression Levels of Nav Subunits during Diabetes

Our study of the expression levels of Nav channels in intact DRG tissues, showed significant decreases in the expression levels of various TTX-S Nav subunits (Nav1.3, Nav1.6 and Nav1.7) one month after STZ-induced diabetes. It is interesting to note that only the TTX-S subunits showed significant decreases in expression levels, while the TTX-R subunits (Nav1.8 and Nav1.9) were unaffected by short-term diabetes. A potential explanation for this selective downregulation of TTX-S subunits would be the significant reduction in the Navβ2 subunit, which has been linked to reduced expression levels of TTX-S Nav subunits (Lopez-Santiago et al., 2006) as will be discussed in this section. Here, we considered the changes in expression levels of the different Nav subunits and possible implications this may entail on DRG neuron excitability.

First, Nav1.3 has been reported to be expressed at practically undetectable levels in adult DRG neurons, but is significantly upregulated after peripheral axotomy or nerve damage (Waxman et al., 1994; Black et al., 1999). Peripheral nerve injuries such as chronic constriction injury, neuroma formation after peripheral nerve transection, and experimental painful diabetic neuropathy cause upregulation of Nav1.3 expression levels (Parnham et al., 2005; Wang et al., 2011). Nav1.3 mediates a TTX-S current that rapidly recovers from inactivation, which is able to support high frequency firing and thus contribute to injury-induced hyperexcitability (Benarroch, 2007). In the present study, we demonstrated a robust expression of Nav1.3 in the DRG of both control and STZ-diabetic mice. We also showed a decrease in Nav1.3 expression one month following STZ-induced diabetes, which could contribute to the reduction in AP firing frequency we have observed in the DRG neurons *in vitro*.

Nav1.6 is reportedly the predominant Nav isoform expressed in the nodes of Ranvier of myelinated sensory axons, as well as along axons of unmyelinated C-fibres (Parnham et al., 2005; Wittmack, 2005; Wang et al., 2011). Hong and Wiley (2004) demonstrated a downregulation in Nav1.6 signal intensities in nodes in diabetic animals, but at the same time an increase in serine/threonine and tyrosine phosphorylation of Nav1.6 (Hong et al., 2004). It has also been reported that p38 phosphorylation of Nav1.6 leads to a significant reduction in Nav1.6 peak current amplitude without any effects on gating properties (Wittmack, 2005). Consequently, p38 phosphorylation of Nav1.6 provides a potential mechanism for slowing nerve conduction in DSN (Tomlinson and Gardiner, 2008). The kinase p38 belongs to the MAPK (mitogen-activated protein kinases) family, which are activated in response to stress. Moreover, the p38 pathway is activated in diabetes and is downstream of the RAGE signalling cascade (Yeh et al., 2001). As mentioned, we recently demonstrated a RAGE-dependent potentiation of capsaicin-evoked currents in DRG neurons exposed to short-term high glucose (Lam et al., 2018). Thus, the RAGE signalling pathway provides a link between Nav subunits and TRPV1 channels that is worth investigating in the future.

Nav1.7 is predominantly expressed in small DRG neurons, and it has been proposed that Nav1.7 may be physiologically coupled to Nav1.8 (Parnham et al., 2005; Wang et al., 2011). Nav1.7 is considered a threshold channel because it amplifies subthreshold stimuli in order to activate

Nav1.8, which is responsible for mediating the majority of Nav currents during the upstroke of an action potential (De Lera Ruiz and Kraus, 2015). Nav1.7 has been implicated in many studies of experimental DPN. Hoeijmakers and colleagues (2014) even proposed that the pathologies of DPN and diabetes occur in parallel with one another. They suggested that both result from mutations in the Nav1.7 gene, which render neurons and pancreatic β cells susceptible to the development of DPN and diabetes, respectively (Hoeijmakers et al., 2014). Moreover, it is well known that mutations in the Nav1.7 gene give rise to a number of pain disorders, including congenital insensitivity to pain, paroxysmal extreme pain disorder, and primary erythromelalgia. The congenital insensitivity to pain results from loss-of-function mutations, while paroxysmal extreme pain disorder and primary erythromelalgia are due to gain-of-function mutations in the Nav1.7 gene (Wang et al., 2011; De Lera Ruiz and Kraus, 2015). Taken together, the central role of Nav1.7 in pain perception suggests a pivotal role in DPN. We observed a decrease in Nav1.7 expression levels one month after STZ-induced diabetes and considering the role of Nav1.7 in other pain disorders, this reduction may potentially contribute to the sensory abnormalities (numbness, weakness and paresthesia) observed in DPN. However, at three months after STZ-induced diabetes, we observed a significant upregulation in Nav1.7, which is consistent with the previous reports on DPN (Hong et al., 2004; Hong and Wiley, 2006).

Nav1.8, along with Nav1.9, are selectively expressed in small DRG neurons (Parnham et al., 2005; Wang et al., 2011). As mentioned above, it has been reported that Nav1.8 carries most of the inward current during the initial spike of the action potential (Yang et al., 2016). Furthermore, under high glucose conditions, there is an increase in the formation of the highly reactive glycolytic metabolite methylglyoxal, which has been proposed to depolarize sensory neurons by inducing posttranslational modifications of Nav1.8 (Bierhaus et al., 2012; De Lera Ruiz and Kraus, 2015). The second TTX-R Nav channel in DRG neurons is Nav1.9, which generates persistent current activated at low voltage thresholds, and thus is believed to contribute to the resting membrane potential (Parnham et al., 2005). One month after induction of diabetes, we did not observe any differences in expression levels of Nav1.8 and Nav1.9 under early diabetic conditions. However, at three months, we observed a trend suggesting an increase in expression levels of these TTX-R subunits. Nav1.8 and Nav1.9 have been implicated in many models of neuropathic pain since they play key roles in the excitability of neurons (Lauria et al., 2014;

Tibbs et al., 2016). Again, similar to Nav1.7, these two Nav isoforms may potentially be contributing to increased pain responses occurring in DSN.

The Navβ2 subunit is covalently linked by a disulfide bond to the α-subunit of Nav channels (Schmidt and Catterall, 1986). Typically, there is a stable free intracellular pool of newly synthesized α-subunit, and disulfide linkage to the Navβ2 subunit is required for its plasma membrane mobilization (Schmidt and Catterall, 1986). $\beta2^{-/-}$ mice display reductions in Nav cell surface expression (Chen et al., 2002). DRG neurons from $\beta2^{-/-}$ mice show reductions in TTX-S Nav currents compared to those from $\beta2^{+/+}$ mice and also show decreased transcripts and protein levels of Nav1.7 (Lopez-Santiago et al., 2006). Lopez-Santiago and colleagues (2006) suggested that the Navβ2 subunit regulates the cell surface expression of TTX-S Nav channels, but not TTX-R Nav channels. Moreover, the upregulation of the Navβ2 subunit in peripheral nerve injury may contribute to hyperexcitability and ectopic firing by recruiting Nav channels to the cell surface (Pertin, 2005). Given this evidence, it is plausible that the decrease in Navβ2 in the present study is responsible for the reductions in the expression levels of the TTX-S subunits (Nav1.3, Nav1.6 and Nav1.7). If this is so, targeting Navβ2 during early DPN could reverse the dysregulation of the involved Nav channels.

Taken together, our study shows changes in the expression levels of Nav subunits that correlate with electrophysiological abnormalities in action potential generation and Na^+ currents in DRG neurons exposed to high glucose conditions. Although we did not correlate these effects of high glucose with pain perception in STZ-diabetic mice, we propose that our finding may contribute to the paradoxical sensation of numbness and loss of perception that can take in place in short-term diabetes (Christianson et al., 2003). Furthermore, our study also revealed that diabetes could affect the expression levels of Nav subunits in different ways depending on the stage of the disease. While we observed a reduction in TTX-S Nav subunit expression at one month of diabetes, this effect was switched to a significant increase in the expression of Nav1.7 at three-month time point. We did not detect significant changes in the expression levels of Nav1.8 and Nav1.9, but rather a seemingly increasing trend, considering that these two Nav isoforms have been implicated in pain abnormalities (Priest et al., 2005; Rush et al., 2006; Bierhaus et al., 2012;

Zhang et al., 2013), future research should be designed to look at the potential change in the expression profile and role of Nav1.8 and Nav1.9 in later stages of DSN.

4.3 Future Directions and Limitations

As mentioned above, a limitation of this study is that we employed neonatal DRG neurons for our *in vitro* studies, while using young adult DRG tissue samples for our western blotting experiments. Our team did try to run western blotting analysis on our cultured DRG samples, but due to low protein concentrations of the Nav subunits in our model, we were unable to detect reliable signals. Instead, we decided to utilize an STZ-diabetic mouse model to validate our *in vitro* findings, and test the relevance of our *in vitro* results in DRG neurons exposed to the host of metabolic insults that occur in diabetes. Moreover, for future studies, it would be interesting to see the functional differences between Nav channels from STZ-induced diabetic and control mice. Secondly, since we observed a decreasing trend for inward currents that are not from Nav channels, it would be worth investigating the roles of T-type calcium channels during the onset of DPN. Tibbs and colleagues (2016) discussed the involvement of voltage-gated Calcium (Ca^{2+}) channels in neuropathic pain. Considering that T-type Ca^{2+} channels Cav3.2 and Cav3.3 are expressed in DRG neurons and may play a role in the pathogenesis of DPN, they may be potential targets to treat DPN.

Finally, our study concentrated on cellular and molecular effects of short-term hyperglycemia in DRG neurons, but to fully understand the relevance of our findings for DPN behavioural studies will be required. Such an approach was beyond the scope of our project, but future research designed to better understand the correlation between changes in Nav channel function and expression with the development of the known DPN symptoms, such as hyperalgesia, allodynia, numbness and loss of pain perception, will shed new light on not only the etiology of this pathology, but also on new therapeutic targets.

REFERENCES

Bach FW, Jensen TS, Kastrup J, Stigsby B, Dejgård A (1990) The effect of intravenous lidocaine on nociceptive processing in diabetic neuropathy. Pain 40:29–34.

Bagal SK, Marron BE, Owen RM, Storer RI, Swain NA (2015) Voltage gated sodium channels as drug discovery targets. Channels 9:360–366.

Bellini S, Barutta F, Mastrocola R, Imperatore L, Bruno G, Gruden G (2017) Heat Shock Proteins in Vascular Diabetic Complications: Review and Future Perspective. Int J Mol Sci 18:1–26.

Benarroch EE (2007) Sodium channels and pain. Neurology 68:233–236.

Bierhaus A et al. (2012) Methylglyoxal modification of Na v 1.8 facilitates nociceptive neuron firing and causes hyperalgesia in diabetic neuropathy. Nat Med 18:926–933.

Black JA, Cummins TR, Plumpton C, Chen YH, Hormuzdiar W, Clare JJ, Waxman SG (1999) Upregulation of a Silent Sodium Channel After Peripheral, but not Central, Nerve Injury in DRG Neurons. J Neurophysiol 82:2776–2785.

Boucek P (2006) Advanced Diabetic Neuropathy: A Point of no Return? Rev Diabet Stud 3:143–150.

Brackenbury WJ, Isom LL (2011) Na+ channel β subunits: Overachievers of the ion channel family. Front Pharmacol 2:1–11.

Brownlee M (2001) Biochemistry and molecular cell biology of diabetic complications. Nature 414:813–820.

Callaghan BC, Cheng HT, Stables CL, Smith AL, Feldman EL (2012) Diabetic neuropathy: Clinical manifestations and current treatments. Lancet Neurol 11:521–534.

Campanucci V, Krishnaswamy A, Cooper E (2010) Diabetes Depresses Synaptic Transmission in Sympathetic Ganglia by Inactivating nAChRs through a Conserved Intracellular Cysteine Residue. Neuron 66:827–834.

Campanucci VA, Krishnaswamy A, Cooper E (2008) Mitochondrial Reactive Oxygen Species Inactivate Neuronal Nicotinic Acetylcholine Receptors and Induce Long-Term Depression of Fast Nicotinic Synaptic Transmission. J Neurosci 28:1733–1744.

Casale R, Symeonidou Z, Bartolo M (2017) Topical Treatments for Localized Neuropathic Pain. Curr Pain Headache Rep 21:1–9.

Catterall WA (1992) Cellular and molecular biology of voltage-gated sodium channels. Am Physiol Soc 72:S15–S46.

Cheing G (2010) Diabetic peripheral neuropathy. Int J Ther Rehabil 17:17–19.

Chen C et al. (2002) Reduced sodium channel density , altered voltage dependence of inactivation , and increased susceptibility to seizures in mice lacking sodium channel β2-subunits. Proc Natl Acad Sci 99:17072–17077.

Chong HL, Ruben PC (2008) Interaction between voltage-gated sodium channels and the neurotoxin, tetrodotoxin. Channels 2:407–412.

Christianson JA, Ryals JM, McCarson KE, Wright DE (2003) Beneficial Actions of Neurotrophin Treatment on Diabetes-Induced Hypoalgesia in Mice. J Pain 4:493–504.

Craner MJ, Klein JP, Renganathan M, Black JA, Waxman SG (2002) Changes of sodium channel expression in experimental painful diabetic neuropathy. Ann Neurol 52:786–792.

De Lera Ruiz M, Kraus RL (2015) Voltage-Gated Sodium Channels: Structure, Function, Pharmacology, and Clinical Indications. J Med Chem 58:7093–7118.

Deeds M, Anderson J, Armstrong A, Gastineau D, Hiddinga H, Jahangir A, Eberhardt N, Kudva Y (2011) Single Dose Streptozotocin Induced Diabetes: Considerations for Study Design in Islet Transplantation Models. Lab Anim (NY) 45:131–140.

Derry S, Wiffen P, Moore R, Quinlan J (2014) Topical lidocaine for neuropathic pain in adults. Cochrane Database Syst Rev.

Dyck PJ, Davies JL, Wilson DM, Service FJ, Melton LJ, O'Brien PC (1999) Risk factors for severity of diabetic polyneuropathy: Intensive longitudinal assessment of the Rochester Diabetic Neuropathy Study cohort. Diabetes Care 22:1479–1486.

Faber CG, Lauria G, Merkies ISJ, Cheng X, Han C, Ahn H-S, Persson A-K, Hoeijmakers JGJ, Gerrits MM, Pierro T, Lombardi R, Kapetis D, Dib-Hajj SD, Waxman SG (2012) Gain-of-function Nav1.8 mutations in painful neuropathy. Proc Natl Acad Sci 109:19444–19449.

Feldman EL, Nave KA, Jensen TS, Bennett DLH (2017) New Horizons in Diabetic Neuropathy: Mechanisms, Bioenergetics, and Pain. Neuron 93:1296–1313.

Gleichmann H, Wang Z (1998) GLUT2 in pancreatic islets: crucial target molecule in diabetes induced with multiple low doses of streptozotocin in mice. Diabetes 47:50.

Goldin AL, Barchi RL, Caldwell JH, Hofmann F, Howe JR, Hunter JC, Kallen RG, Mandel G, Meisler MH, Netter YB, Noda M, Tamkun MM, Waxman SG, Wood JN, Catterall WA (2000) Nomenclature of Voltage-Gated Sodium Channels. Neuron 28:365–368.

Graham ML, Janecek JL, Kittredge JA, Hering BJ, Schuurman HJ (2011) The streptozotocin-induced diabetic nude mouse model: Differences between animals from different sources. Comp Med 61:356–360.

Hirade M, Yasuda H, Omatsu-Kanbe M, Kikkawa R, Kitasato H (1999) Tetrodotoxin-resistant sodium channels of dorsal root ganglion neurons are readily activated in diabetic rats. Neuroscience 90:933–939.

Hodgkin A, Huxley A (1952). A Quantitative Description of Membrane Current and its Application to Conduction and Excitation in Nerve. J Physiol 117:500–544.

Hoeijmakers JGJ, Faber CG, Merkies ISJ, Waxman SG (2014) Channelopathies, painful neuropathy, and diabetes: Which way does the causal arrow point? Trends Mol Med 20:544–550.

Hogan Q (2010) Labat Lecture: The Primary Sensory Neuron: Where it is, What it Does, and Why it Matters. Reg Anesth Pain Med 35:306–311.

Hong S, Morrow TJ, Paulson PE, Isom LL, Wiley JW (2004) Early painful diabetic neuropathy is associated with differential changes in tetrodotoxin-sensitive and -resistant sodium channels in dorsal root ganglion neurons in the rat. J Biol Chem 279:29341–29350.

Hong S, Wiley JW (2006) Altered expression and function of sodium channels in large DRG neurons and myelinated A-fibers in early diabetic neuropathy in the rat. Biochem Biophys Res Commun 339:652–660.

Jeffcoate WJ, Harding KG (2003) Diabetic foot ulcers. Lancet 361:1545–1551.

Jin HY, Park TS (2017) Role of inflammatory biomarker in diabetic peripheral neuropathy. J Diabetes Investig:2017–2019.

Kandel ER, Schwartz JH, Jessell TM, Siegelbaum SA, Hudspeth AJ (2013) Principles of Neural Science, Fifth Edition. United States of America: McGraw-Hill Companies, Inc.

Kaur S., Pandhi P., Dutta P. (2011) Painful diabetic neuropathy: An update. Ann Neurosci 18:168–175.

Kharatmal SB, Singh JH, Sharma SS (2015) Comparative evaluation of in vitro and in vivo high glucose-induced alterations in voltage-gated tetrodotoxin-resistant sodium channel: Effects attenuated by sodium channel blockers. Neuroscience 305:183-196.

Kobayashi M, Zochodne DW (2018) Diabetic neuropathy and the sensory neuron: New aspects of pathogenesis and their treatment implications. J Diabetes Investig 9:1239–1254.

Krames ES (2014) The role of the dorsal root ganglion in the development of neuropathic pain. Pain Med 15:1669–1685.

Lai J, Porreca F, Hunter JC, Gold MS (2004) Voltage-Gated Sodium Channels and Hyperalgesia. Annu Rev Pharmacol Toxicol 44:371–397.

Lam D, Momeni Z, Theaker M, Jagadeeshan S, Yamamoto Y, Ianowski JP, Campanucci VA (2018) RAGE-dependent potentiation of TRPV1 currents in sensory neurons exposed to high glucose. PLoS One 13:1–23.

Lauria G, Ziegler D, Malik R, Merkies ISJ, Waxman SG, Faber CG (2014) The Role of Sodium Channels in Painful Diabetic and Idiopathic Neuropathy. Curr Diab Rep 14.

Lopez-Santiago LF, Pertin M, Morisod X, Chen C, Hong S, Wiley J, Decosterd I, Isom LL (2006) Sodium Channel 2 Subunits Regulate Tetrodotoxin-Sensitive Sodium Channels in Small Dorsal Root Ganglion Neurons and Modulate the Response to Pain. J Neurosci 26:7984–7994.

Louraki M, Karayianni C, Kanaka-Gantenbein C, Katsalouli M, Karavanaki K (2012) Peripheral neuropathy in children with type 1 diabetes. Diabetes Metab 38:281–289.

Mao J, Chen LL (2000) Systemic lidocaine or mexiletine for neuropathic pain. Pain 87:7–17.

Namadurai S, Yereddi NR, Cusdin FS, Huang CLH, Chirgadze DY, Jackson AP (2015) A new look at sodium channel β subunits. Open Biol 5:140192

Nascimento AI, Mar FM, Sousa MM (2018) The intriguing nature of dorsal root ganglion neurons: Linking structure with polarity and function. Prog Neurobiol 168:86–103.

Ogurtsova K, da Rocha Fernandes JD, Huang Y, Linnenkamp U, Guariguata L, Cho NH, Cavan D, Shaw JE, Makaroff LE (2017) IDF Diabetes Atlas: Global estimates for the prevalence of diabetes for 2015 and 2040. Diabetes Res Clin Pract 128:40–50.

Pabbidi RM, Yu SQ, Peng S, Khardori R, Pauza ME, Premkumar LS (2008) Influence of TRPV1 on diabetes-induced alterations in thermal pain sensitivity. Mol Pain 4:1–17.

Parnham M, Coward K, Baker MD (2005) Sodium Channels, Pain, and Analgesia. Birkhäuser Verlag.

Patel NJ, Llewelyn JG, Wright DW, Thomas PK (1994) Glucose and leucine uptake by rat dorsal root ganglia is not insulin sensitive. J Neurol Sci 121:159–162.

Pertin M (2005) Upregulation of the Voltage-Gated Sodium Channel 2 Subunit in Neuropathic Pain Models: Characterization of Expression in Injured and Non-Injured Primary Sensory Neurons. J Neurosci 25:10970–10980.

Pop-Busui R, Boulton AJM, Feldman EL, Bril V, Freeman R, Malik RA, Sosenko JM, Ziegler D (2017) Diabetic neuropathy: A position statement by the American diabetes association. Diabetes Care 40:136–154.

Priest BT, Murphy BA, Lindia JA, Diaz C, Abbadie C, Ritter AM, Liberator P, Iyer LM, Kash SF, Kohler MG, Kaczorowski GJ, MacIntyre DE, Martin WJ (2005) Contribution of the tetrodotoxin-resistant voltage-gated sodium channel NaV1.9 to sensory transmission and nociceptive behavior. Proc Natl Acad Sci 102:9382–9387.

Ragsdale DS, Mcphee JC, Scheuer T, Catterall WA (1994) Molecular Determinants of State-Dependent Block of Na+ Channels by Local Anesthetics. Science (80-) 265:1724–1728.

Renganathan M, Cummins TR, Waxman SG (2017) Contribution of Nav1.8 Sodium Channels to Action Potential Electrogenesis in DRG Neurons. J Neurophysiol 86:629–640.

Rigon F, Rossato D, Auler VB, Bosco LD, Partata WA (2013) Effects of sciatic nerve transection on ultrastructure , NADPH-diaphorase reaction immunoreactivities in frog dorsal root ganglion. Brazilian J Med Biol Res 46:513–520.

Rush AM, Cummins TR, Waxman SG (2007) Multiple sodium channels and their roles in electrogenesis within dorsal root ganglion neurons. J Physiol 579:1–14.

Rush AM, Dib-Hajj SD, Liu S, Cummins TR, Black JA, Waxman SG (2006) A single sodium channel mutation produces hyper- or hypoexcitability in different types of neurons. Proc Natl Acad Sci 103:8245–8250.

Russell JW, Sullivan KA, Windebank AJ, Herrmann DN, Feldman EL (1999) Neurons undergo apoptosis in animal and cell culture models of diabetes. - Abstract - UK PubMed Central. Neurobiol Dis 6:347–363.

Said G (2007) Diabetic neuropathy - A review. Nat Clin Pract Neurol 3:331–340.

Sapunar D, Kostic S, Banozic A, Puljak L (2012) Dorsal root ganglion - A potential new therapeutic target for neuropathic pain. J Pain Res 5:31–38.

Sayir F, Kavak S, Meral I, Demir H, Cengiz N, Çobanoğlu U (2013) Effects of crush and axotomy on oxidative stress and some trace element levels in phrenic nerve of rats. Brain Res Bull 92:84–88.

Schmidt JW, Catterall WA (1986) Biosynthesis and processing of the α subunit of the voltage-sensitive sodium channel in rat brain neurons. Cell 46:437–445.

Simpson IA, Dwyer D, Malide D, Moley KH, Travis A, Vannucci SJ (2008) The facilitative glucose transporter GLUT3: 20 years of distinction. Am J Physiol Metab 295:E242–E253.

Smith AG, Ramachandran P, Tripp S, Singleton JR (2001) Epidermal nerve innervation in impaired glucose tolerance and diabetes-associated neuropathy. Neurology 57:1701–1704.

Stino AM, Smith AG (2017) Peripheral neuropathy in prediabetes and the metabolic syndrome. J Diabetes Investig 8:646–655.

Sumner CJ, Sheth S, Griffin JW, Cornblath DR, Polydefkis M (2003) The spectrum of neuropathy in diabetes and impaired glucose tolerance. Neurology 60:108–111.

Suo M, Wang P, Zhang M (2016) Role of Fyn-mediated NMDA receptor function in Prediabetic Neuropathy in Mice. J Neurophysiol:jn.00229.2016.

Szallasi A, Cortright DN, Blum CA, Eid SR (2007) The vanilloid receptor TRPV1: 10 years from channel cloning to antagonist proof-of-concept. Nat Rev Drug Discov 6:357–372.

Szkudelski T (2001) The mechanism of alloxan and streptozotocin action in B cells of the rat pancreas. Physiol Res 50:537–546.

Tesfaye S et al. (2010) Diabetic neuropathies: Update on definitions, diagnostic criteria, estimation of severity, and treatments. Diabetes Care 33:2285–2293.

The Diabetes Control and Complications Trial Research Group (1993) The Effect of Intensive Treatment of Diabetes on the Development and Progression of Long-Term Complications in Insulin-Dependent Diabetes Mellitus. N Engl J Med 327:669–677.

Thornalley PJ (2002) Glycation in diabetic neuropathy: characteristics, consequences, causes, and therapeutic options. Int Rev Neurobiol 50:37–57.

Tibbs GR, Posson DJ, Goldstein PA (2016) Voltage-Gated Ion Channels in the PNS: Novel Therapies for Neuropathic Pain? Trends Pharmacol Sci 37:522–542.

Tomlinson DR, Gardiner NJ (2008) Glucose neurotoxicity. Nat Rev Neurosci 9:36–45.

Uemura E, Greenlee HW (2006) Insulin regulates neuronal glucose uptake by promoting translocation of glucose transporter GLUT3. Exp Neurol 198:48–53.

Vincent AM, Perrone L, Sullivan KA, Backus C, Sastry AM, Lastoskie C, Feldman EL (2007) Receptor for advanced glycation end products activation injures primary sensory neurons via oxidative stress. Endocrinology 148:548–558.

Vinik AI, Park TS, Stansberry KB, Pittenger GL (2000) Diabetic neuropathies. Diabetologia 43:957–973.

Wang W, Gu J, Li Y-Q, Tao Y-X (2011) Are Voltage-Gated Sodium Channels on the Dorsal Root Ganglion Involved in the Development of Neuropathic Pain? Mol Pain 7:1744-8069-7–16.

Waxman SG (2012) Sodium channels, the electrogenisome and the electrogenistat: Lessons and questions from the clinic. J Physiol 590:2601–2612.

Waxman SG, Dib-Hajj SD, Cummins TR, Black JA (1999) Sodium channels and pain. Proc Natl Acad Sci 96:7635–7639.

Waxman SG, Kocsis JD, Black JA (1994) Type III Sodium Channel mRNA Is Expressed in Embryonic But Not Adult Spinal Sensory Neurons, and Is Reexpressed Following Axotomy. J Neurophysiol 72:466–470.

Wilson ML (2017) Prediabetes: Beyond the Borderline. Nurs Clin North Am 52:665–677.

Wittmack EK (2005) Voltage-Gated Sodium Channel Nav1.6 Is Modulated by p38 Mitogen-Activated Protein Kinase. J Neurosci 25:6621–6630.

Wood JN, Boorman JP, Okuse K, Baker MD (2004) Voltage-gated sodium channels and pain pathways. J Neurobiol 61:55–71.

Yang L, Li Q, Liu X, Liu S (2016) Roles of voltage-gated tetrodotoxin-sensitive sodium channels NaV1.3 and NaV1.7 in diabetes and painful diabetic neuropathy. Int J Mol Sci 17:1–10.

Yeh C, Sturgis L, Haidacher J, Zhang X, Sherwood SJ, Bjercke RJ, Juhasz O, Crow MT, Tilton RG, Denner L (2001) Requirement for p38 and p44/p42 Mitogen-Activated Protein Kinases in RAGE-Mediated Nuclear Factor-?B Transcriptional Activation and Cytokine Secretion. Diabetes 50:1495–1504.

Zhang XY et al. (2013) Gain-of-Function mutations in SCN11A cause familial episodic pain. Am J Hum Genet 93:957–966.

APPENDIX A
COPYRIGHT PERMISSIONS

Figure 1.1 was adapted from "Kandel ER, Schwartz JH, Jessell TM, Siegelbaum SA, Hudspeth AJ (2013) Principles of Neural Science, Fifth Edition. United States of America: McGraw-Hill Companies, Inc.", with permission from McGraw Hill Companies.

Figure 1.2 was reproduced from "Benarroch EE (2007) Sodium channels and pain. Neurology 68:233–236", with permission from Wolters Kluwer Health, Inc.

Figure 1.3 was adapted from "Bagal SK, Marron BE, Owen RM, Storer RI, Swain NA (2015) Voltage gated sodium channels as drug discovery targets. Channels 9:360–366.". It is under a Creative Commons Attribution-Non-Commercial License http://creativecommons.org/licenses/by-nc/3.0/

Copyright Clearance Center

Confirmation Number: 11841342
Order Date: 08/13/2019

Customer Information

Customer: Maricris Bautista
Account Number: 3001480605
Organization: University of Saskatchewan
Email: mnb633@usask.ca
Phone: +1 (306) 491-0981
Payment Method: Invoice

This is not an invoice

Order Details

Principles of neural science

Billing Status: **N/A**

Order detail ID: 71979814
ISBN: 9780071390118
Publication Type: Book
Publisher: MCGRAW-HILL
Author/Editor: KANDEL, ERIC R.

Permission Status: **Granted**
Permission type: Republish or display content
Type of use: Republish in a thesis/dissertation
Order License Id: 4647290897953

Requestor type	Academic institution
Format	Electronic
Portion	image/photo
Number of images/photos requested	1
The requesting person/organization	Maricris Bautista
Title or numeric reference of the portion(s)	Figure 24-4 B. Convergence of visceral and somatic afferent fibres....
Title of the article or chapter the portion is from	Chapter 24 Pain
Editor of portion(s)	Allan I. Basbaum and Thomas M. Jessell
Author of portion(s)	Allan I. Basbaum and Thomas M. Jessell
Volume of serial or monograph	n/a
Page range of portion	535
Publication date of portion	2013
Rights for	Main product
Duration of use	Current edition and up to 5 years
Creation of copies for the disabled	no

With minor editing privileges	no
For distribution to	Canada
In the following language(s)	Original language of publication
With incidental promotional use	no
Lifetime unit quantity of new product	Up to 499
Title	EFFECT OF SHORT-TERM DIABETES ON THE EXPRESSION AND FUNCTION OF TETRODOTOXIN-SENSITIVE VOLTAGE-GATED SODIUM CHANNELS IN MOUSE SENSORY NEURONS
Institution name	n/a
Expected presentation date	Aug 2019

Note: This item was invoiced separately through our **RightsLink service.** More info **$ 0.00**

Total order items: 1 **Order Total: $0.00**

WOLTERS KLUWER HEALTH, INC. LICENSE TERMS AND CONDITIONS

Jul 18, 2019

This Agreement between University of Saskatchewan -- Maricris Bautista ("You") and Wolters Kluwer Health, Inc. ("Wolters Kluwer Health, Inc.") consists of your license details and the terms and conditions provided by Wolters Kluwer Health, Inc. and Copyright Clearance Center.

The publisher has provided special terms related to this request that can be found at the end of the Publisher's Terms and Conditions.

License Number	4632060768307
License date	Jul 18, 2019
Licensed Content Publisher	Wolters Kluwer Health, Inc.
Licensed Content Publication	Neurology
Licensed Content Title	Sodium channels and pain
Licensed Content Author	Eduardo E. Benarroch
Licensed Content Date	Jan 16, 2007
Licensed Content Volume	68
Licensed Content Issue	3
Type of Use	Dissertation/Thesis
Requestor type	Individual
STM publisher name	
Portion	Figures/table/illustration
Number of figures/tables/illustrations	1
Figures/tables/illustrations used	Figure
Author of this Wolters Kluwer article	No
Title of your thesis / dissertation	EFFECT OF SHORT-TERM DIABETES ON THE EXPRESSION AND FUNCTION OF TETRODOTOXIN-SENSITIVE VOLTAGE-GATED SODIUM CHANNELS IN MOUSE SENSORY NEURONS
Expected completion date	Aug 2019
Estimated size(pages)	60
Attachment	PR57-397_BAUTI_190716.pdf
Requestor Location	University of Saskatchewan 614 Pichler Crescent Saskatoon, SK S7V 0G2 Canada Attn: University of Saskatchewan
Billing Type	Invoice

Billing Address	University of Saskatchewan 614 Pichler Crescent Saskatoon, SK S7V 0G2 Canada Attn: University of Saskatchewan
Total	0.00 USD

Terms and Conditions

Wolters Kluwer Health Inc. Terms and Conditions

1. **Duration of License:** Permission is granted for a one time use only. Rights herein do not apply to future reproductions, editions, revisions, or other derivative works. This permission shall be effective as of the date of execution by the parties for the maximum period of 12 months and should be renewed after the term expires.
    i. When content is to be republished in a book or journal the validity of this agreement should be the life of the book edition or journal issue.
    ii. When content is licensed for use on a website, internet, intranet, or any publicly accessible site (not including a journal or book), you agree to remove the material from such site after 12 months, or request to renew your permission license
2. **Credit Line:** A credit line must be prominently placed and include: For book content: the author(s), title of book, edition, copyright holder, year of publication; For journal content: the author(s), titles of article, title of journal, volume number, issue number, inclusive pages and website URL to the journal page; If a journal is published by a learned society the credit line must include the details of that society.
3. **Warranties:** The requestor warrants that the material shall not be used in any manner which may be considered derogatory to the title, content, authors of the material, or to Wolters Kluwer Health, Inc.
4. **Indemnity:** You hereby indemnify and hold harmless Wolters Kluwer Health, Inc. and its respective officers, directors, employees and agents, from and against any and all claims, costs, proceeding or demands arising out of your unauthorized use of the Licensed Material
5. **Geographical Scope:** Permission granted is non-exclusive and is valid throughout the world in the English language and the languages specified in the license.
6. **Copy of Content:** Wolters Kluwer Health, Inc. cannot supply the requestor with the original artwork, high-resolution images, electronic files or a clean copy of content.
7. **Validity:** Permission is valid if the borrowed material is original to a Wolters Kluwer Health, Inc. imprint (J.B Lippincott, Lippincott-Raven Publishers, Williams & Wilkins, Lea & Febiger, Harwal, Rapid Science, Little Brown & Company, Harper & Row Medical, American Journal of Nursing Co, and Urban & Schwarzenberg - English Language, Raven Press, Paul Hoeber, Springhouse, Ovid), and the Anatomical Chart Company
8. **Third Party Material:** This permission does not apply to content that is credited to publications other than Wolters Kluwer Health, Inc. or its Societies. For images credited to non-Wolters Kluwer Health, Inc. books or journals, you must obtain permission from the source referenced in the figure or table legend or credit line before making any use of the image(s), table(s) or other content.
9. **Adaptations:** Adaptations are protected by copyright. For images that have been adapted, permission must be sought from the rightsholder of the original material and the rightsholder of the adapted material.
10. **Modifications:** Wolters Kluwer Health, Inc. material is not permitted to be modified or adapted without written approval from Wolters Kluwer Health, Inc. with the exception of text size or color. The adaptation should be credited as follows: Adapted with permission from Wolters Kluwer Health, Inc.: [the author(s), title of book, edition, copyright holder, year of publication] or [the author(s), titles of article, title of journal, volume number, issue number, inclusive pages and website URL to the journal page].
11. **Full Text Articles:** Republication of full articles in English is prohibited.
12. **Branding and Marketing:** No drug name, trade name, drug logo, or trade logo can be included on the same page as material borrowed from Diseases of the Colon & Rectum, Plastic Reconstructive Surgery, Obstetrics & Gynecology (The Green Journal), Critical Care Medicine, Pediatric Critical Care Medicine, the American Heart Association publications and the American Academy of Neurology publications.

13. **Open Access:** Unless you are publishing content under the same Creative Commons license, the following statement must be added when reprinting material in Open Access journals: "The Creative Commons license does not apply to this content. Use of the material in any format is prohibited without written permission from the publisher, Wolters Kluwer Health, Inc. Please contact permissions@lww.com for further information."
14. **Translations:** The following disclaimer must appear on all translated copies: Wolters Kluwer Health, Inc. and its Societies take no responsibility for the accuracy of the translation from the published English original and are not liable for any errors which may occur.
15. **Published Ahead of Print (PAP):** Articles in the PAP stage of publication can be cited using the online publication date and the unique DOI number.
    i. Disclaimer: Articles appearing in the PAP section have been peer-reviewed and accepted for publication in the relevant journal and posted online before print publication. Articles appearing as PAP may contain statements, opinions, and information that have errors in facts, figures, or interpretation. Any final changes in manuscripts will be made at the time of print publication and will be reflected in the final electronic version of the issue. Accordingly, Wolters Kluwer Health, Inc., the editors, authors and their respective employees are not responsible or liable for the use of any such inaccurate or misleading data, opinion or information contained in the articles in this section.
16. **Termination of Contract:** Wolters Kluwer Health, Inc. must be notified within 90 days of the original license date if you opt not to use the requested material.
17. **Waived Permission Fee:** Permission fees that have been waived are not subject to future waivers, including similar requests or renewing a license.
18. **Contingent on payment:** You may exercise these rights licensed immediately upon issuance of the license, however until full payment is received either by the publisher or our authorized vendor, this license is not valid. If full payment is not received on a timely basis, then any license preliminarily granted shall be deemed automatically revoked and shall be void as if never granted. Further, in the event that you breach any of these terms and conditions or any of Wolters Kluwer Health, Inc.'s other billing and payment terms and conditions, the license is automatically revoked and shall be void as if never granted. Use of materials as described in a revoked license, as well as any use of the materials beyond the scope of an unrevoked license, may constitute copyright infringement and publisher reserves the right to take any and all action to protect its copyright in the materials.
19. **STM Signatories Only:** Any permission granted for a particular edition will apply to subsequent editions and for editions in other languages, provided such editions are for the work as a whole in situ and do not involve the separate exploitation of the permitted illustrations or excerpts. Please view: STM Permissions Guidelines
20. **Warranties and Obligations:** LICENSOR further represents and warrants that, to the best of its knowledge and belief, LICENSEE's contemplated use of the Content as represented to LICENSOR does not infringe any valid rights to any third party.
21. **Breach:** If LICENSEE fails to comply with any provisions of this agreement, LICENSOR may serve written notice of breach of LICENSEE and, unless such breach is fully cured within fifteen (15) days from the receipt of notice by LICENSEE, LICENSOR may thereupon, at its option, serve notice of cancellation on LICENSEE, whereupon this Agreement shall immediately terminate.
22. **Assignment:** License conveyed hereunder by the LICENSOR shall not be assigned or granted in any manner conveyed to any third party by the LICENSEE without the consent in writing to the LICENSOR.
23. **Governing Law:** The laws of The State of New York shall govern interpretation of this Agreement and all rights and liabilities arising hereunder.
24. **Unlawful:** If any provision of this Agreement shall be found unlawful or otherwise legally unenforceable, all other conditions and provisions of this Agreement shall remain in full force and effect.

For Copyright Clearance Center / RightsLink Only:

1. **Service Description for Content Services:** Subject to these terms of use, any terms set forth on the particular order, and payment of the applicable fee, you may make the following uses of the ordered materials:

i. **Content Rental:** You may access and view a single electronic copy of the materials ordered for the time period designated at the time the order is placed. Access to the materials will be provided through a dedicated content viewer or other portal, and access will be discontinued upon expiration of the designated time period. An order for Content Rental does not include any rights to print, download, save, create additional copies, to distribute or to reuse in any way the full text or parts of the materials.

ii. **Content Purchase:** You may access and download a single electronic copy of the materials ordered. Copies will be provided by email or by such other means as publisher may make available from time to time. An order for Content Purchase does not include any rights to create additional copies or to distribute copies of the materials

Other Terms and Conditions:

Questions? customercare@copyright.com or +1-855-239-3415 (toll free in the US) or +1-978-646-2777.